RHICAGR a Most Simplified RHIC Lattice

A. G. Ruggiero

August 1991

Collider Accelerator Department

Brookhaven National Laboratory

U.S. Department of Energy

USDOE Office of Science (SC)

DISCLAIMER

Accelerator Physics Technical Note No. 26

RHICAGR
A Most Simplified RHIC Lattice

A.G. Ruggiero

August 1991

RHICAGR

A Most Simplified RHIC Lattice

A.G. Ruggiero

Accelerator Development Department
Brookhaven National Laboratory
August 12, 1991

Mea Non Culpa

In this report I describe an alternative *approach* to the design of the RHIC lattice. It is not my intention to propose an alternative lattice altogether, but I like to stress the differences in design methodology and philosophy. RHICAGR is an example of lattice I have produced in a very short period of time (months) where I wanted to include what in my judgment is relevant and to exclude features I have never concurred with in the RHIC91 design. The new lattice carries my initials because indeed it has been the intense effort of a single person, essentially ignored during the development of RHIC91. If the design considerations were evaluated or accepted at the proper time, probably there would never have been a RHICAGR but a more simplified RHIC91 (recently a committee called that RHIC91').

There are several considerations in this report which reflect my judgment and evaluation of the RHIC project accumulated during the last several years. There are features and requirements in the RHIC design which are conflicting and extreme. They do not represent a challenge in the scientific sense; working with them is tedious and very little rewarding. But I believe it is important that the limitations are assessed and emphasized. I feel I have an obligation to the community to keep it informed of any finding and uneasiness encountered in the design development.

I hope that this work has made somebody reflect and ponder on the direction we are embarking. If somebody will get upset reading my report, I will not apologize, I will be content to have reached a goal. If even one of my recommendations or suggestions made in this report is accepted and followed I will consider the work successful.

Contents

1. Motivation

For several reasons, which I do not believe it is necessary to list here, I set up myself on a quest: the search for a most simplified RHIC lattice. Notice that I preferred to say *a most* and not *the most* because I am aware that once the design principles involved in the discussion that follows have been accepted, there is room for further improvement and refinement and that other lattice solutions satisfying those principles may be found.

My major motivation and concern is the derivation of a lattice which allows simplicity in being tuned during the commissioning and the early stage of operation. I believe that this can be accomplished only if very few parameters are involved; these parameters should be clearly identified, their range and function specified. Some of them will provide dispersion control, others the low-beta configuration at the crossing regions, whereas few more will adjust phase-advance and global betatron tunes. In my opinion an orthogonal setting of *knobs* is highly desirable so that when some of them are varied for a specific function the other basic features of the lattice are not altered too appreciably.

The RHIC is made of superconducting magnets which are known to be susceptible to very large regular and skew quadrupole errors. During the commissioning period of the collider it may not be possible to correct for the consequences of these errors without having first tuned the lattice to allow a circulating beam. The lattice distortions during that period can be very large; for instance they could cause a beta-function mismatch around the ring as large as 100%. Even after correction, once a circulating beam has been established, because the number of correctors is less than the number of the magnets bearing the errors, an appreciable lattice distortion remains; for instance one can expect a residual beta- function mismatch of about 10%. Similarly the RHIC lattice will exhibit a dispersion fluctuation, both horizontally and vertically, which at the start can be as large as a fraction to a whole meter, to be reduced later to 10-20 cm after subsequent correction. Moreover, even with a perfect lattice an uncertainty of few percents will remain on the determination of the lattice functions due to the inherent measurement errors.

The RHIC lattice should be simple and flexible, capable to absorb the uncertainties and errors of the lattice functions. A too rigid lattice, which is designed disregarding these assumptions, may require too many conditions and too many parameters in order to satisfy

excessive matching requirements. I feel that RHIC91 is in that regard a very rigid lattice,* with a very unclear plan for tuning. The insertions of this lattice are designed with so many conditions all overlapping each other. As an example, all eighteen quadrupoles are involved in the dispersion matching and control of the dispersion at the crossing region, and at the same time all the same quadrupoles do other functions too.

---

* RHIC91 is the latest version of a lattice proposed for RHIC based on design principles with roots in the ISABELLE/CBA design and carries still now some of the features of those times, for instance the presence of some special dipoles in the insertions. The work was initially carried out by J. Claus and later by S.Y. Lee who changed the initial symmetric insertion to an anti-symmetric configuration. The latest version is the result of alternating and/or common effort of J. Claus, S.Y. Lee and S. Tepikian. The latter is at the moment the depositary of the results of the work.

2. Design Requirements

Several requirements nevertheless have to be satisfied in the design of the RHIC lattice. These requirements are set up in front together with the motivation and the goal of the project. They are listed below with definitions and comments drawn from my own judgment and interpretation:

1. The RHIC lattice has to fit the CBA tunnel. Many of us consider a fortune to have a tunnel for the RHIC project already available on site. Yet it is not normal procedure in the accelerator design business that a lattice has to tailor the geometry of an existing tunnel. Certainly this was done for Tevatron, and it is been done also for the LHC in CERN. But one should be aware that in order to follow the geometry of a tunnel one is also accepting some limitations on the freedom of the design.

   Nevertheless, fortunately, the CBA tunnel has generous, wide dimensions which can be used to allow movement of the lattice sidewise up to about a meter on either side. One can use in principle this allowance as long as the magnets remain physically in the tunnel and are easily reachable. There are no reasons why one should insist on keeping the ring lattice very close to the center of the tunnel.

2. The RHIC is made of two superconducting rings intersecting with each other and both rings are accommodated in the same tunnel. Two configurations are possible. In one, horizontal, the two rings are side-by-side and each beam moves from an *inner* arc to an *outer* arc periodically, crossing horizontally the other beam in the intersection regions. This geometry clearly imposes the existence of two basically different arcs. In the second choice, vertical, the two magnet rings are on top of each other which requires only one type of arc with no distinction between *top* or *bottom* arc except location. Each beam would then move periodically from the top to the bottom arc crossing vertically with the other beam.

   At a certain point there should have been a discussion on the issue of which is the better configuration, horizontal versus vertical. It is unfortunate that this

never happened. When I tried to raise it a couple of times years ago, I was given two lines of reasoning. I was told of the existence of a *theorem* by which the vertical layout of the two rings is excluded. This could have been true for the ISABELLE or CBA type of collider where the beams are continuous with large horizontal width and narrow height which require crossing at large horizontal angle. But with RHIC we are dealing with a more efficient type of collider with head-on collision of bunched round beams. That *theorem* does not apply to RHIC. The second explanation was even more curious, I remember it was too late to make a change (also at that time!), it was said, because all the magnet design and engineering was already too far developed...

I believe the issue is important and deserves a discussion no matter how far we are in the construction of the project, even if, for some contingent reasons, choices have been made. Depending on the philosophical approach of the lattice design, the vertical layout could actually be preferred if one insists on the preservation of matching of the lattice functions to the highest degree.

3. There are six arcs and six long straight sections. This is not a choice but a constraint caused by the shape of the tunnel inherited from the ISABELLE/CBA times. If one could start from fresh ground, very likely would choose two or four or may be even eight interaction regions; or would opt for a cluster configuration as in the SSC design. These options are not available to RHIC.

4. There should be allowance for injection and there should be allowance for beam abort. Yes, but only once per beam! RHIC91 has been designed essentially with the capability built in the lattice to inject and abort at every long straight. Adding to the low-beta at the interaction region and to the beam crossing requirements, all this makes quite a challenging lattice to design. It is unfortunate that RHIC does not allow for utility insertions like in Tevatron, Sp$\overline{\text{p}}$S and SSC where the functions of injection and abort are separated from those of low-beta insertions.

Because of limitation of economic and human resources, for many years the RHIC will be exploited by as few as two experiments. These two experiments

will occupy two of the six long straights leaving the other four unused, at least for a long time. Because of the facility already available and also inherited from the ISABELLE/CBA times, one of these experiments, with high performance goals, will occupy the 6 o'clock region. This is an unfortunate situation, because it is there where also injection into both rings occur, and where beam abort from both rings has been shown on the charts. Until recently the design of the RHIC91 lattice has been made difficult by the burdens imposed on the design of the 6 o'clock region.

One could accept the fact that RHIC91 does not allow for utility insertions. Yet four of the six long straights will remain unused for a long time. I believe that it is considerably better, easier and more economical if the four unused long straights are bridged with regular FODO cells of little impact or optimal consequences to the overall lattice. They can always be replaced in a (distant) future with low-beta insertions when necessary.

5. Each interaction region has to be tunable from a large value of β^* to allow for injection and acceleration, to a small value. Until recently the range of $\beta^* = 2$ to 6 m has been required for the baseline design. But a wider range from $\beta^* = 1$ m to at least 10 m seems more desirable. It should be understood that this tunability is required with the beam circulating and thus therefore must be continuous and smooth. Finally a ± 10 m magnet free region around the crossing point has been imposed on the design. This is a severe condition since it places the two innermost quadrupoles (Q1) at 50 m distance from each other, compared to 40 m in the SSC.

3. The Vertical Layout

The most preferable configuration for RHIC is the vertical layout, where the two rings are on top of each other and each beam moves alternatively from a bottom to a top arc and crosses with the other beam vertically, as it has been proposed for the SSC. The two arcs are identical and the quadrupole arrangement may be chosen with a perfect periodicity six: each period with a mirror symmetry. The same periodicity and symmetry is preserved also by the distribution of the arc dipoles. To provide crossing at an angle and collision between unequal species, the special dipoles at the insertions have an anti-symmetric arrangement from the bending point of view and basically establish a periodicity of three which nevertheless only locally distorts the periodicity of six of the rest of the lattice. The focusing of the insertion dipoles has a mirror symmetry and is consistent with the six-fold periodicity. Of course I am assuming that all the interaction regions are developed and designed in the same way; otherwise the periodicity is broken to essentially one-fold though high degree of internal symmetry still remain.

The vertical layout has the least number of parameters involved: a significant simplification for design, book-keeping, survey and lattice analysis. It is easier to commission and to operate. If indeed matching of the lattice functions should be important and must be obtained to a very high accuracy, the vertical configuration allows that with the least number of parameters.

There are two consequences for the design of the RHIC lattice when the vertical configuration is adopted. In the arcs there is an horizontal dispersion due to the bending in the horizontal plane; on the other hand the vertical crossing is obtained with bending in the vertical direction which introduces thus a vertical dispersion. It is mandatory to separate the origin and the propagation of the two types of dispersion. This can be accomplished with a dispersion killer insertion at both ends of each arc so that the dispersion is effectively brought to zero in both planes as one leaves an arc and approaches the crossing region proper. Here, the vertical dispersion appears with the first dipole used to provide the crossing. The vertical dispersion is required to vanish again as one leaves the last dipole for crossing. The separation of the horizontal from the vertical dispersion can be accomplished with modularity built in the design of the lattice as done for instance in

the SSC lattice. It is then clearly seen that whereas the horizontal dispersion originating from the arcs has a symmetric behavior around the crossing point, the vertical dispersion from the insertion itself has an anti-symmetric behavior. This of course is true also in the horizontal configuration of the two rings where the crossing region now creates locally an horizontal dispersion. This is indeed very apparent also in RHIC91 where confusion between the two sources is nevertheless introduced by the absence of modularity in the design plan.

The proper way for the local control of the dispersion due to a crossing geometry is to separate each set of dipoles at the two sides of the crossing by a $M = -1$ insertion, for instance two 90° phase-advance FODO cell, as it is done in the design of the SSC lattice. Unfortunately this requires too much space and cannot be accommodated in the RHIC. The only alternative I found, which is described later, is a symmetric low-beta insertion, whereas the method used in the SSC can allow also an anti-symmetric insertion.

Because of the mirror symmetry around the crossing point, the arcs, if they are made of a whole number of regular FODO cells, begins and ends with quadrupoles of the same polarity which I have chosen here to be QD.

I do not like there to make an issue of symmetric versus anti-symmetric insertions, but my instinctive preference is for an anti-symmetric one because provides automatically cancellation of the contributions to the natural chromaticity of the two sides of an insertion, whereas these contributions add in the case of a symmetric insertion. I did not choose a symmetric configuration intentionally; I have been rather forced to it by the considerations I just made.

4. Procedure

I urge that the vertical layout for RHIC is given very serious consideration. But I can understand that *now* we are indeed too far in the development of the magnet acquisition. Then I have come up with the following procedure.

I begin first with the design of the RHIC lattice with a vertical layout. This involves only one type of arc made of twelve regular FODO cells from QD to QD. The insertion is modular and of the same type everywhere except for the bending sign of the innermost dipoles which alternates from insertion to insertion. The design of this type of lattice requires indeed only very few parameters and provides *exact* matching of the lattice functions everywhere.

In a second step, I rotate the magnet arrangement from vertical to horizontal, creating thus an inner and outer arc, and an inner and outer half-insertion. But in this operation I provide only for the required adjustment in the length of the drifts and leave all the setting for the magnets unchanged, including the gradient of the quadrupoles in both the arcs and insertions. In principle this operation is also used in the RHIC91 lattice design where one first works around an *average* arc and then the arcs at the two sides, leaving only one type of QF and one type of QD quadrupoles. This approach nevertheless was not used consistently in the design of the insertion.

After the transformation from vertical to horizontal configuration is done, I record the effects due to the rotation, for instance the amount of lattice distortions introduced. It is remarkable how little mismatch is generated, well within those caused by errors, corrected or not, or by measurement uncertainties.

5. Features

I did not want to create too much deviation from the RHIC91 lattice, thus I have adopted the same FODO cell with only one dipole between quadrupoles and 90° phase advance in both planes. There are twelve regular cells in each arc; but, as I have said, each arc begins with a QD and ends with a QD. I found the long straight in RHIC too long and I wanted to continue beyond the arc still with more regular FODO cells, including the dispersion killer sections, as far as I could go towards the crossing region. Also when bending dipoles disappear, I tried to preserve the distance between QF and QD as in the arcs. This simplifies considerably the power supply arrangement, as well as that of magnets and cryostats.

As in RHIC91, the dipoles are centered exactly in the regular FODO cells, halfway between quadrupoles. This configuration provides a waist in the middle of the QD quadrupoles and helps to reduce the amount of lattice distortions.

The horizontal dispersion is suppressed with the conventional method of placing dipole magnets in proper location without having to change the gradient of quadrupoles. In principle this method works effectively for a given horizontal phase-advance in the regular FODO cell. I will show that the dispersion killing function is very little upset during the β^* tuning and the change of the global betatron tunes. It is the modular feature of the design which indeed makes the lattice less sensitive to changes.

RHIC91 has been advertised as needing the regulation of all eighteen quadrupoles in the insertion in addition of the regular QF and QD in the arcs, to get a perfect tuning and matching. If the philosophical approach outlined here is followed, then by requiring that the nine inner quadrupoles are set at the same excitation of the nine outer quadrupoles, like it is done for QF and QD in the inner and outer arcs, a lattice mismatch will result of only one to two percent. Moreover the lattice I am describing (RHICAGR) has already the dispersion adjusted properly and as a consequence I will need two *knobs* less than of the original nine.

There is one more difference. The design of RHIC91 insists on the exact determination of the phase-advance across the insertion in both planes and requires that it is fixed to given values. The betatron tunes are then obtained by varying QF and QD in the arcs

accordingly. I believe that this procedure is not realistic. Because of the errors and uncertainties one cannot rely on the determination and adjustment of the phase-advance across the insertion to good accuracy. Thus I have removed also these conditions. When I tune the insertion to change β^* I take whatever phase-advance will result across and readjust QF and QD to obtain the desired betatron tunes. This is a procedure that is easier to follow and closer to the one will be adopted during actual commissioning and operation of the collider. The same will be done when one desires to change the global tunes for fixed insertions: again only QF and QD will be varied.

The entire tunability of RHICAGR, the lattice I am proposing for RHIC, requires as few as five quadrupole-knobs in the insertions, Q1 through Q5, in addition to QF and QD. I have proven that the range of tunability is larger and easier than the one demonstrated with RHIC91. The behavior is smooth and continuous and absorbs very well uncertainties and errors. The amount of distortion introduced in the lattice functions does not exceed a couple of percent over the entire range explored.

6. Description of the RHICAGR Lattice

The horizontal layout of the collider is shown in Fig. 1. It applies to both RHIC91 and RHICAGR. The separation between the axis of the two beams is 90 cm. Each long straight is 283.5 m long. The major difference in the two lattices is the average radius of the arcs; this will be discussed more in detail later when the location of the two rings in the tunnel is examined. Because of the difference introduced by the inner and outer arc, the periodicity is three-fold. But in the case of RHICAGR this is only a minor perturbation to the more basic six-fold periodicity. Moreover RHICAGR has a mirror symmetry around both each crossing point and the arc bisectors.

The regular FODO cell in the arcs is described in Fig. 2. All the parameters are shown there. The dipole magnet is placed exactly halfway between the two quadrupoles. This is a common feature to both lattices. The drifts (D) at both sides have the lengths listed. The reader certainly can notice the duplication in the book-keeping required by the horizontal layout. For reasons that will be explained later, the dipole magnet has a field of 3.32 T for the rigidity of 839.5 T·m corresponding to 100 GeV/u kinetic energy for Au-ions. This field is about 4% lower than in RHIC91 and helps to widen the safety margin between the nominal operation value and the quenching level. As a consequence, also the bending radius and the bending angle have values altered by that amount.

Half of a long straight section is shown in Fig. 3. The end of the arc is followed by a Dispersion Killer which is made also of two regular FODO cells. The dispersion is controlled by locating properly the two short dipoles (B2) around the QF quadrupoles. This adjustment is minor but can be accommodated only for a given phase-advance in the horizontal plane across the regular FODO cell; once this is set, the position of those dipoles is also fixed and cannot be varied any longer. Both dispersion and dispersion derivative are effectively brought to zero at the end of the last regular dipole (B), and will remain zero up to the first crossing dipole (BC3). In the arcs and in the Dispersion Killer sections only two sets of regular quadrupoles are required, QF and QD, all of the same type #1 described later. QDK is a special quadrupole of type #2 of large aperture which occurs only once over the twelve equivalent locations, to allow for beam injection, otherwise is a regular QD quadrupole of type #1. I have proven that interchanging length with gradient

at the QDK location does not upset the lattice behavior at all. This is an indication of a well-behaving lattice; a feature that sometimes failed in RHIC91.

The Dispersion Killer section is followed by the interaction region proper. The modularity of insertion design is obvious. There are two functions provided by the interaction regions: a low-beta insertion with a five-quadrupole *telescope*, and the beam crossing with three special dipoles. I shall describe each of them next with some details.

The scheme which provides beam crossing is described in Fig. 4. It is made of three dipoles on each side of the crossing point; BC1, the innermost, is identical to the one also used in RHIC91. Three of the five telescope quadrupoles, Q1, Q2 and Q3 are located between BC2 and BC3.

The two beams are *parallel* and separated by 90 cm up to BC3 which is constantly set to the same field value of the regular dipoles (B). The beam axis is always at the center of Q1, Q2 and Q3 and never changes. The crossing angle capability, between zero and 6.6 mrad, is provided between BC2 and BC1 by varying their field. The path length will vary minimally in BC2 and BC1 as the crossing angle is changed. The path lengths, bending angles and other parameters shown in Fig. 4 correspond to zero crossing angle.

The only way to compensate for the dispersion created by the crossing dipoles is to place the quadrupole triplet between them. Ideally one would need an $M = -1$ insertion so that the dispersion is effectively confined between BC3 and BC2. Unfortunately, there is not enough space for this in RHIC, and the alternative solution is to require zero dispersion at the crossing point but a finite derivative. In this way the dispersion remains confined between BC3 and BC3 and is zero outside. BC1 is a special dipole with about 19 mrad bending angle. The geometry forces for an entrance angle also of the same amount which thus creates a significant focusing with a noticeable effect on the dispersion behavior. Overall the crossing dipole configuration provides a symmetric focusing function, especially at the entrance of BC1. This fact then seems to impose a symmetric low-beta insertion.

The low-beta insertion is provided by a *telescope* which is a sequence of five quadrupoles. The front end of the telescope is made of the triplet Q1-Q2-Q3 and the *ocular* by the doublet Q4-Q5 at the back. The analogy to an optical telescope is obvious. Like in the analog, the *objective* made of the triplet stays fixed aiming at the object, whereas the two knobs in the back, Q4 and Q5, vary their gradient in opposite direction, to provide the focusing.

I have opted for a relative *long telescope* but I have experimented also with a *short* one, as that shown in Fig. 5. A short telescope is made of more powerful lenses, but it is considerably more stable compared to the long one. By this I mean that of course solutions can be found for both of them, but with the short telescope, like in the similar optical analogy, the search for the solution can be found easily with less sensitivity to errors since it provides a wider aperture. The long telescope is more difficult to tune and basically more unstable and more sensitive to errors; on the other side the lenses are weaker and cheaper, again, like in the optical analog. The solution I have chosen employs the same number of quadrupoles in the insertion as RHIC91.

For comparison, the layout of the insertion for RHIC91 is shown in Fig. 6 which is more or less on the same scale of Figs. 3 and 5. From the comparison between Figs 3 and 6, that is RHICAGR versus RHIC91, several different features emerge. Also RHIC91 employs a telescope made of the sequence of Q1-Q5, but it is even a longer telescope with the *ocular* Q4 and Q5 too close to each other. The motivation has been to provide a long drift free of magnets for beam dump. Unfortunately, this telescope configuration is more unstable and requires very careful tuning on the computer; very little errors or deviations will grossly upset the focusing. In order to provide for the dispersion matching and the adjustment of the phase-advance across the insertion, four more quadrupoles on each side are added, Q6 to Q9, which interfere with the function of the telescope itself.

Observe that the triplet Q1-Q2-Q3 is about the same and is at the same location in both lattices; Q4 and Q5 are too far out in RHIC91 compared to those in RHICAGR; Q6 and Q7 are just about at the same location, whereas Q8 has been shifted in RHICAGR halfway between Q9 and Q7. Thus, actually, the quadrupole configuration in the two lattices is not very different; but the same differences I believe are very important and should be closely examined.

There is no effective dispersion killing in RHIC91. The one and one-half dipoles in the long straight, between Q7 and Q5 are those inherited from the ISABELLE/CBA times, and are now needed to match the geometry of the CBA tunnel. The equivalent of these dipoles in RHICAGR acquire the function to cancel the dispersion from the arcs. Their location is different and there is one extra half-length dipole for each dispersion killer. This modifies somewhat the location of the two rings in the tunnel but still in a very acceptable

manner, as I shall show later. Moreover the bending of each arc is effectively increased by the addition of the equivalent one full length dipole; this, in my opinion, makes a more efficient use of the tunnel, which has too long straight sections, and lower the bending field significantly by about 4%.

By far the most important difference in the two layouts is how the two beams are brought crossing with each other. There are no quadrupoles between BC1 and BC2 in RHIC91 and this unfortunately creates a significant interference between the dispersion from the arcs and that generated by the crossing itself, with all the consequences I have discussed before.

7. The $\beta^* = 2$ m Lattice (RHICAGR)

Now that all the pieces have been put together, the next step is the determination of $\beta^* = 2$ m lattice with the same configuration in all six crossing regions. The method I followed to obtain this is the following:

1. I work on the *average* lattice, with the same inner and outer arc and identical sides of the long straight section. Eventually this corresponds to the vertical layout, depending on the rotation of the dipole magnets at the crossing region.

2. I start imposing $\Delta Q_H = \Delta Q_V = 0.25$, that is exactly 90° as the phase-advance across the regular FODO cell in the arc.

3. I derive the gradients G_F and G_D of the regular quadrupoles QF and QD to satisfy point #2 (or #8, see below).

4. I work out a sequence of 12 FODO cells, the arc, which are all exactly matched to each other, after cycling, and I derive all the lattice functions in the middle of the last QD.

5. I add the dispersion killer section, made of two regular FODO cells in sequence without the last QD quadrupole. I adjust by a little amount the drifts between the special, short dipoles B2 at both sides of QF until I obtain zero dispersion with vanishing derivative at the exit of the last regular dipole (B).

6. Tracking the lattice functions from the end of the arc, obtained as explained in #4, going through the dispersion killer section, the telescope and the crossing region, I match half of the insertion to the crossing point. I vary the gradients of the five telescope quadrupoles Q1 through Q5 to satisfy the following conditions

$$\beta_H^* = \beta_V^* = 2m$$

$$\alpha_H^* = \alpha_V^* = X_p^* = 0.0$$

At this stage I do not impose any particular condition of the maximum value of β that I might encounter either in Q2 or Q3.

7. I estimate the total betatron tunes Q_H and Q_V for the whole ring.

8. I readjust the phase-advances ΔQ_H and ΔQ_V across the regular FODO cells in the arcs to accommodate for the excess or defects between the desired betatron tune values and those measured as indicated in point #7. For this purpose

I spread the differences among 96 regular FODO cells and assume that the telescope regions between Q5 quadrupoles do not essentially give contribution to the total betatron tunes.

9. I repeat steps #3 through #8 iteratively.

This method is very effective and converges in very few iterations. The result is a perfectly matched lattice with periodicity six and mirror symmetry around the crossing point and the middle of the arc. As a result

$$\Delta Q_H = 0.2452$$

$$\Delta Q_V = 0.2594$$

From now on the phase advances across the regular FODO cells are left unchanged and consequently also the location of the two special dipoles (B2) for the dispersion killing is frozen. It is during this stage that the actual location of the five telescope quadrupoles is varied to find the most suitable solution within limits imposed by engineering considerations on the length of drifts. After this step also the location of these quadrupoles of course remains unchanged. An inspection of the lattice shows that the maximum value of beta is 615 m in the horizontal plane at Q2. This lattice constitutes the starting point for the search of subsequent lattices with different β^* values and different betatron tunes. The method of tunability will be explained later, but I have also used it to generate a slightly different $\beta^* = 2$ m lattice as it can be obtained from a realistic *beta-squeeze* from the $\beta^* = 6$ m value used in the injection mode. After expanding this lattice to an horizontal configuration with inner and outer arcs, by readjusting the drift lengths where necessary, and leaving the gradient of all the quadrupoles unchanged, the maximum value of beta has increased to 630 m and shifted to the vertical plane at Q3.

The general parameters of this lattice are listed in Table 1. The betatron tunes have now a difference of six units, which could be lowered to five if required. The fractional parts of the betatron tunes are about those proposed in RHIC91. The transition energy is essentially unchanged, since all the major modifications are in the insertion. The natural chromaticity is somewhat higher, thirty units in the horizontal plane more than in RHIC91. This is the only negative sign I could observe for RHICAGR; it is due to the nature of the symmetric insertion. But it is an effect that I believe, as I will show later, one can still cope with reasonably well.

Table 1: General Parameters.

β^*	2 m
Circumference	3833.8450 m
Average Radius	610.1754 m
Bending Radius	253.1137 m
Q_H	34.82489 (33.846)
Q_V	28.82433 (28.830)
Transition Energy, γ_T	24.76
ξ_H	-104.25
ξ_V	-78.47

Mismatch	Inner	Outer
$(\Delta\beta/\beta)_H$ @ QF	$\pm$ 0.003	$\pm$ 0.0002
$(\Delta\beta/\beta)_V$ @ QD	$\pm$ 0.003	$\pm$ 0.0002
X_p @ QD	1.52–1.57 m	

The amount of lattice distortion, due to the splitting of the average lattice in the outer and inner layouts, measured by the mismatch factors also shown in Table 1, is less than one percent both in β and dispersion. Thus, to me, the horizontal layout of the RHIC is an acceptable configuration.

Finally I would like to point out a negative feature which is due to the peculiarity of the tunnel geometry and thus in common to all lattices for RHIC. The dipole bending radius and the collider average radius are both shown in Table 1. The ratio of these two quantities, called the *packing factor*, has a physical significance in the sense that underlies the amount of lattice irregularities, difficult to correct, like natural chromaticity, due to the long straight sections, compared to the amount available in a regularly behaving lattice, like the arcs, where correction schemes and correctors are located. For RHIC91 the packing

factor is 39%, for RHICAGR 41%. These quantities should be compared to 61% for the LHC, 73% for the SSC and 75% for Tevatron and Sp$\bar{\text{p}}$S.

The dispersion behavior of RHICAGR is shown in Fig. 7. One can clearly see the dispersion from the arc to be effectively killed and followed by a region with zero dispersion. At the same time the dispersion from the insertion is small, localized and shows an anti-symmetry behavior around the crossing point.

The lattice envelop functions β_H and β_V are shown in Fig. 8. Again I would like to stress how I managed to keep the behavior of these functions under control and smooth, like that in the arcs, all the way up to the telescope region, where the insertion proper takes place.

8. Magnet Components

The quadrupole list for RHICAGR is given in Table 2. There are three types: 1, 2 and 3. Figure 3 shows the distribution and location of the quadrupoles according to their type. Type #1 is made of the regular QF and QD quadrupoles in the arcs and dispersion killers, with the exception of one location where injection occurs (see later) which requires a large aperture quadrupole of type #2; this is the one listed in Fig. 3 as QDK. Of the five quadrupoles which make the telescope, Q5 is also a type #1 quadrupole whereas Q4 is a strong magnet which therefore I have made it long and chosen it of the type #3 which has also large aperture. The large aperture of Q4 is also required, at least in one place, to allow for beam abort as it is discussed later in this report. The quadrupoles in the triplet are all of large aperture type: Q1 and Q3 of type #2 and Q2, like Q4, of type #3.

Table 2: Quadrupole List for RHICAGR.

Type #	1	2	3
Length (m)	1.13	1.45	2.25
Bore (mm)	80	130	130
Number/Ring	197	25	24
Location	QF,QD,Q5	QDK,Q1,Q3	Q2,Q4

Table 3 gives the list of all the dipole magnets involved in RHICAGR. One can see that there are three types. Type #1 includes the regular dipole (B) and those in the dispersion killer sections (B2); they have 80 mm bore, of the same cross-section design, and can all be set on the same power supply bus. The second type of dipoles includes BC3 that has a large bore to avoid a too severe physical aperture limitation. BC3 is located in places where the two beams are already separated by 90 cm. The third type is made of BC1, a special type of magnet indeed, common to both RHICAGR and RHIC91. A special case is the BC2 dipole which is very difficult to build with a large aperture. Like in RHIC91 also here for RHICAGR I have no choice but to make BC2 of the type #1. As it can be seen in Fig. 4, the BC2 magnets must be separated for both beams so that their physical separation is an issue for engineering design. An important parameter is the displacement

of the beam axis in front of BC2 from the median plane. This displacement for RHICAGR is 189 mm.

Table 3: The Dipole List for RHICAGR.

Type #		1		2	3
Dipole	B	B2	BC2	BC3	BC1
Bending Radius (m)		253.1137		253.1137	196.4348
Bore (mm)		80		130	200
Field (T)		3.32		3.32	4.3
Length (m)	9.45	4.84	1.3622	3.4054	3.7
No./Ring	156	24	12	12	–
No./RHIC	–	–	–	–	12

In principle the magnet aperture should be chosen to avoid limitations on the physical betatron acceptance around the ring. A summary of the effects of the magnet aperture is shown in Table 4. For each magnet we list the maximum β-value corresponding to a $\beta^* = 2$ m lattice; in parenthesis whether the maximum occurs in the horizontal (H) or vertical (V) plane or in both; the bore diameter; and the acceptance defined as

$$\text{Acceptance} = \left(\frac{1}{2} \text{ bore} - 4 \text{ mm} \right)^2 / \beta$$

The betatron acceptance in the arcs does not change with β^* and should be taken as the reference. There is a limitation to 6 πmm·mrad at Q2 and Q3 which appears also in RHIC91. A serious bottleneck is BC2 which yields to an acceptance of 5.4 πmm·mrad for RHICAGR and even less, 5.0 πmm·mrad, for RHIC91 since in this lattice $\beta = 260$ m. The limitation at BC3 is removed since it is possible to make it with a larger bore. The issue of BC1, I prefer here not to touch.

Table 4: Physical Acceptance for RHICAGR.

Magnet	β	bore	Acceptance
	m	mm	πmm·mrad
QF	50.7 (H)	80	25
QD	50.1 (V)	80	25
Q1	297 (H)	130	12.5
Q2	588 (H)	130	6.3
Q3	630 (V)	130	5.9
Q4	103 (H)	130	36.
Q5	93 (V)	80	14.
BC1	93 (H&V)	200	–
BC2	241 (H&V)	80	5.4
BC3	384 (V)	130	9.7

9. Fitting the CBA Tunnel with RHICAGR

It is important to prove that the RHICAGR lattice can fit comfortably well in the CBA tunnel. Magnets should be easily installed and easily reachable, at least from one side.* Figure 9 is the latest version of the ring/tunnel geometry which is proper to RHIC91. The date says July 91 and the location of *injection* and *dump* are shown at Q6. The relevant parameters which determine the location of the magnets in the tunnel are the distance of the crossing point from the center and the distance of the middle point of the average arc from the center.

Both lattices have a periodicity of six from the geometry point of view which greatly simplifies installation and survey. The major parameters are given in Table 5. Notice that even RHIC91 lattice is not quite centered to the tunnel enclosure; in the arc there is a difference of about 2.3 cm to the inside, whereas in the straight enclosure the difference is 16 cm to the outside. In RHICAGR these differences are larger and in the same direction: 73 cm in the middle of the arcs to the inside, and 128 cm in the straight enclosure to the outside. These are the locations with the largest deviations; at the entrance and exit of the arcs the deviations are the smallest, and actually the RHICAGR lattice sits just at the center of the tunnel as shown in Fig. 10. The location of the magnets in the tunnel in the middle of the arc is shown in Fig. 11, and the corresponding location at the crossing point in Fig. 12. It is seen that there are no impediments of significance and that installation and replacement of magnets can be engineered with no great difficulties.

Table 5: Major Geometrical Parameters.

	Middle of Arc (Average) to Center	Crossing Location to Center
Tunnel	620.8847 m	590.3298 m
RHIC91	620.8619	590.4912
RHICAGR	620.1544	591.6098
RHICAGR-Tunnel	−0.73 m	+1.28 m

10. The Beta-Squeeze

The tunability of the RHICAGR lattice is very effective, as I am going to demonstrate next, over a very large range. The starting point is the $\beta^* = 2$ m lattice I have described earlier. Reversing the procedure, which corresponds to reality when from an injection lattice with large β^* value one tunes the collider to a lower value, it is required to change β^* at the crossing point in small steps leaving the global betatron tunes and all other parameters unchanged. The method I have used is just an example, very simple, fast and effective. More elaborate schemes could also be proposed, with the same philosophical approach.

Suppose I got a solution during the n-th iteration described by β_n^* which I use as the start for the next iteration to get $\beta_{n+1}^* = \beta_n^* + \Delta$. All the work is done with the average lattice, and as usual, the effects on a realistic lattice with split arcs are later recorded.
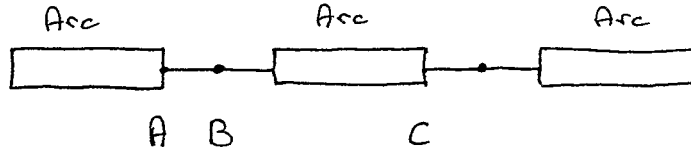
With reference to the figure, I perform the following three steps:

1. Track the lattice functions from A to B. The lattice functions at A are those obtained in the previous iteration, denoted by A_n, after cycling as usual the whole period from A to C. By varying the five quadrupoles in the telescope I impose the solution B_{n+1} at B which is made of the four conditions $\beta_H^* = \beta_V^* = \beta_{n+1}^*$ and $\alpha_H^* = \alpha_V^* = 0$ and skip over, for simplicity, the condition $X_P^* = 0$.

2. Adjust the global phase advance in both planes between A and C, the whole period, to the original values. This is done by varying QF and QD in the arcs and dispersion killer cells. The assumption is that the change in the phase advance has occurred in the insertion and that can be compensated simply by the arc.

3. With the new setting values of all the quadrupoles involved, I finally recycle the period between A and C to obtain the new initial conditions A_{n+1}, to be used for the next β^* change. Before, though, the three steps are iterated few times to obtain convergency. This appears to be very fast and effective.

This method has been used to vary β^* from 2m to 6m in steps of 0.5 m, and from 6m to 16m in steps of 2m. Once the *injection* value $\beta^* = 6$m is reached, the process is inverted again, as one would do in reality, to recover the $\beta^* = 2$m lattice. Also in this process I did not make use of the $X_p^* = 0$ condition, but approaching the $\beta^* = 2$m value I found necessary to set the limit of 630 m on the maximum value of β_V at Q3. This is the lattice which I have described before, summarized in Table 1 and Figs. 7 and 8. Following the same direction, but removing now also the $\beta_{\max}$ condition, I could obtain lattices for $\beta^* = 1.5$ and 1.0 m.

The dispersion behavior for $\beta^* = 1.0$ and 16 m is shown respectively in Figs. 13 and 14. Though I did not make use of the condition $X_p^* = 0$, the behavior of the dispersion is still very close to the original with not much upset. This feature, I claim, is due to the modularity of the lattice design. The largest deviation is of course for $\beta^* = 16$ m where $X_p^* = 0.13$ m and still with good behaviors in the arcs.

Figures 15 and 16 show the β-functions respectively for $\beta^* = 1$ and 16 m. The maximum value encountered for β is 1250 m, shifted to Q2 and in the horizontal plane. The interesting feature is that during the tuning only that part of the lattice in the telescope region changes, whereas outside it has the same stable behavior of the regular FODO cells.

The variation needed of the quadrupole gradients to cover the range $\beta^* = 1$ to 16 m is shown in Fig. 17 and 18. Like QD, also the gradient of QDK is held essentially constant to the value which is 1.13/1.45 times the gradient of QD. Figures 19 to 23 show the behavior of several lattice characteristics during the beta-squeeze. Since I did not deliberately impose the condition $X_p^* = 0$ during the procedure, it is reasonable to check the results and see if they are acceptable. Both Figs. 20 and 22 indicate very marginally upsetting conditions.

Overall the lattice is responding remarkably well to tuning. Another figure of merit is the lattice mismatch caused by both the presence of inner and outer arc and by the peculiar method of tuning. The amount of mismatch is described in Figs. 24 to 26. The β- distortion is a fraction of a percent in the horizontal plane and less than 2% in vertical one. Larger is the range of the dispersion distortion mostly due to the method of tuning I have chosen. Likely, an improved procedure which imposes also the $X_p^* = 0$ condition would reduce the amount of distortion.

11. Betatron Tuning

In the following exercise, I started with the $\beta^* = 2$ m lattice and wanted to vary the global betatron tune by one unit downward in the horizontal plane, while keeping the vertical tune unchanged. I used a routine similar to the one for the beta-squeeze, where the same unchanged conditions for the crossing region were used, again excluding the $X_p^* = 0$ condition. The result of the procedure is described in Fig. 27 which shows the actual variation of the betatron tunes in the tune diagram. The variation demanded was in steps of 0.2 for the tune change. The final values have a fractional part very close to those at start as it was required. On the side of the diagram I show the required setting of the QF and QD quadrupoles. The QD gradient did not change appreciably, whereas the relative change of the QF gradient was proportional to the relative change of the horizontal betatron tune. During this operation the gradients of the other quadrupoles did not change at all as shown in Fig. 28. Thus I made a second test where I kept constant the five telescope quadrupoles and varied QF and QD gradients just enough to obtain the required change in betatron tunes from the arcs alone (and dispersion killer cells). The result was the same: again, a merit of the modularity employed in the lattice, and a proof that requiring a constant phase-advance across the straight sections is not needed. During the second test I checked the variation of the dispersion in the crossing region and at Q4 and Q5 to detect any upsetting of the dispersion killer. The results are shown in Fig. 29.

12. Chromaticity Studies

I can see only two negative points in the performance of the RHICAGR lattice and both are the result of the use of a symmetric insertion. This type of insertion does not allow common quadrupoles, which is a choice one makes contingent to the need of the project, and contributes to a large natural chromaticity which can be investigated and the consequences determined. In this sense an anti-symmetric insertion is preferable, but, as I will show, also the large chromaticity in RHICAGR can be coped with reasonably well. Fig. 30 displays the uncorrected chromaticity versus β^*; for $\beta^* = 2$ m, the horizontal value is 50% larger than the corresponding value for RHIC91.

I should point out that S.Y. Lee has written a report* recently where he values the merits of a lattice similar to RHICAGR and correctly stress the problems one may encounter with correcting the chromaticity. Unfortunately he left with a negative note implying that probably a correction is impossible. I am very appreciative of his work but I would like to remove here his objection. The natural chromaticity of the RHICAGR lattice is correctable! and this fact indeed removes one of my major points of concern when I was forced to adopt a symmetric insertion.

For simplicity, I am placing sextupoles in the center of the regular quadrupoles QF and QD. Like in RHIC91, they are located only by the arc quadrupoles: there are twelve in each arc next to QD and twelve next in QF. I start first with two sextupole families, SF, next to QF, and SD, next to QD. Their integrated gradient in order to correct chromaticity to zero in both planes are

$$\frac{B''\ell}{B\rho} = 0.27 \text{ for SF}$$
$$= -0.46 \text{ for SD}$$

well within the correctors capability. The behavior of the corrected chromaticities is shown in Fig. 31. The operation of the collider with $\beta^* = 2$ m is really possible only at top energy, 100 GeV/u for beam of Au-ions, and it is doubtful that more than two of the six crossing regions will be indeed operating at $\beta^* = 2$ m. Thus the case we are considering is pessimistic. Yet the full beam momentum spread is only $\pm$ 0.2% and the full beam emittance 0.7 πmm·mrad.

---

* S.Y. Lee, "Properties of a Symmetric RHIC Insertion", BNL-46416, AD/RHIC-101, BNL July 1991.

Over such a small momentum spread, two sextupole families is then adequate since the tune variation is 0.006 in the horizontal plane and considerably less in the vertical. Also the tune-spread for the emittance quoted due to the aberration effect is less than 0.003 in the horizontal plane and negligible in the vertical plane.

My judgment is that one should consider a wider momentum spread, for instance $\pm$ 0.5%. In this case the vertical chromaticity is still well behaving and flat, but the horizontal chromaticity shows a parabolic or cubic tendency for positive values of the momentum error δ. It is possible to express the dependence of tunes δ with a Taylor expansion up to cubic order

$$\Delta Q_H = \xi_H \delta + Q_x'' \delta^2 + Q_x''' \delta^3 + \cdots$$

$$\Delta Q_V = \xi_V \delta + Q_y'' \delta^2 + Q_y''' \delta^3 + \cdots$$

There are six parameters involved which require six sextupole families to flatten the dependence of the tunes with momentum up to third-order. I have been debating with myself* on the best way of grouping sextupole in six families and instead I have come up with the following scheme of eight families.
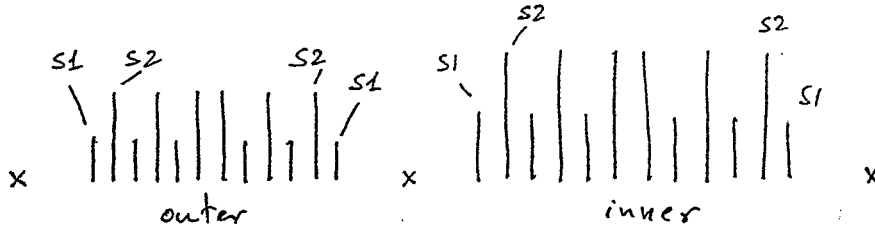
They are spread over a period including an outer and an inner arc. I believe that within each arc there should be a symmetric arrangement, and I allowed that the settings in the inner and outer arcs to be different. The chromaticities with eight sextupole families is shown in Fig. 32. I varied the mutual strength so to leave always the following conditions satisfied

$$Q_x''' = 0$$

$$Q_y'' = Q_y''' = 0$$

I allowed the parabolic term Q_x'' to vary as shown. There are indeed very significant effects and compensations. For instance I believe the case with $Q_x'' = 1300$ is very acceptable. Over the momentum spread of $\pm$ 0.5% the horizontal tune change is 0.015 and less in the

---

vertical plane. The tune spread due to the aberration effects did not change appreciably from the case of two sextupole families and it is thus negligible.

I am positive that given time other combinations can be found with even better performance. Here, I did not try to improve on the solution I quickly found. Fig. 33 to 37 explore the dependence of the lattice function in several critical locations of the lattice with the momentum error δ. All the results shown are valid for the eight sextupole families described above.

Finally I converted to the lattice with $\beta^* = 2$ m and a depressed horizontal tune by one unit. I left the sextupole arrangement *unchanged* and obtained the chromatic behavior shown in Fig. 38. In conclusion, despite the fact that the natural chromaticity is higher, it is nonetheless correctable. This result makes the symmetric insertion more appealing to me. There has been even time to do some modest tracking on the computer.* The sextupoles were set to the eight-family configuration specified above and no other errors were included. Only tracking on momentum ($\delta = 0$) was done for the $\beta^* = 2$ m case. The results are shown in Fig. 39 with the results for RHIC91 in the background. Three runs were made: the dynamical aperture was established with the sextupoles on and essentially no physical limitations. The value 12 mm at the center of QF, is shown on the chart as a blank circle. The physical aperture with sextupoles (denoted by ⊠) was determined by surrounding the beam with a physical enclosure to represent the local vacuum chamber. The value for RHICAGR is 12 mm and is somewhat larger than the value of 7-8 mm for RHIC91; but in the latter case the higher order multiple errors were also included. Finally the physical aperture without sextupoles was determined and it is even larger than the RHIC91 result. As also already concluded for RHIC91 "the study concluded that the physical aperture of the BC2 dipole represents the limiting factor".

---

* The tracking studies for RHICAGR were done by J. Milutinovic using PATRIS.

13. Beam Injection

The person who is developing a lattice has also the task to insure the possibility of injection and abort. I do not believe in the separation of the tasks. The work has to be done coherently with the same style and approach. The lattice designer has the methods and the perception to move things around to accommodate other functions. Henceforth I also wanted myself to find and to prove a method for beam injection in the lattice I am proposing. In the next section I will expose my own thoughts on beam dump.

There are several ways one can design the dispersion killer at the ends of the arcs. The one I have chosen allows what in my judgment is the most effective way of beam injection. I should say in the meantime that I have never been satisfied with the method of injection proposed in RHIC91. Figure 40 compares side by side the layout of the two lattices in the region of injection. Both of them employs an injection kicker (vertical) next to the same quadrupole that in RHIC91 is called Q9 and in RHICAGR is a regular QD. The magnet upstream is nevertheless different. It is an horizontal bending Lambertson magnet for RHICAGR and a vertical septum magnet for RHIC91. The most effective way for injection is a sequence of an horizontal bend followed by a vertical kick or viceversa, a vertical bend followed by an horizontal kick. Since the injection kicker is located next to a defocusing quadrupole, this makes it a vertical kicker. The use of a Lambertson has considerable benefits over a septum magnet: it avoids the use of current carrying separators and does not need to be pulsed. In any case the location of the Lambertson or septum magnet is different in the two schemes. The septum magnet in RHIC91 is located between Q7 and Q8 which is a too tight space and requires both Q7 and Q8 to be *warm* magnets. The septum magnet is too much against Q7 creating some difficulty in the engineering. Moreover the phase advance between septum magnet and kicker is not optimized.

The solution I have adopted places the Lambertson magnet back just beyond QDK, the large aperture quadrupole meant for injection. This solution allows optimum phase advance between kicker and Lambertson since they are exactly one regular FODO cell a part. There is room behind the Lambertson for the beam to be taken horizontally away and clear the nearest QF quadrupole sidewise. Figure 41 shows the location of the *injected* vacuum chamber with respect to that quadrupole. All the magnets involved are *cold* since

there is enough separation between magnets to install cold-to-warm transition. The kicker and Lambertson magnets are obviously warm. All the magnets on the path have regular aperture, except QDK. Figure 42 gives more details of the layout with all the drifts involved. A sketch of the cross-section of the structure at the end of the Lambertson facing QDK is shown in the left-bottom corner. The betatron acceptance injected is 3 πmm·mrad, whereas the circulating betatron acceptance is 20 πmm·mrad, somewhat less than that in the regular arcs (see Table 4) but considerably larger than 6 πmm·mrad allowed in RHIC91. The separation between the two beam axis is 50 mm. The sketch (and it should be taken as such: a sketch) shows the apertures and beam dimensions in scale and hints to the possibility of the design of the Lambertson *lips* with enough gap to allow the passage of the injected beam without encountering any obstruction.

Finally there is the issue of matching and of taking the beam from the new location of the Lambertson to the transfer line toward the AGS. One should take into account the different geometry of RHICAGR and its fitting in the CBA tunnel. The work* was done by J. Xu who demonstrated the transfer and the matching to very good accuracy. The subsequent dipole magnets in the transfer line need to lower their bending field by 4%. Table 6 gives the summary of the vertical kicker parameter and Table 7 that for the horizontal Lambertson. These magnets are relatively easy and do not represent major engineering challenge.

---

* J. Xu, RHIC/AP Technical Note 94.

Table 6: Injection Kicker Magnet.

Effective Length	4.5 m
Field	300 Gauss
Kick Angle	1.3 mrad
Aperture (H×V)	50×70 mm^2
Risetime	80 nsec
Current Stability	1%
β_V at Center	32 m

Table 7: Horizontal Lambertson Magnet.

Effective Length	5.0 m
Field	0.8 T
Bending Radius	125 m
Kick Angle	40 mrad
β_V at QDK side	40 m
Current Stability	0.1%

14. Beam Abort

The same considerations apply to the design of the beam abort. Not even a month ago RHIC 91 was plagued by the design of the 6 o'clock insertion. There was still struggling to get the aborted beam through a sequence of four magnets, and, moreover, in the wrong direction, toward the experimental area.

The best solution is to take the beam straight away with a kicker and to let it travel over a long drift until it clears physically the next magnet down the line. This simple solution requires a very powerful kicker and a very long drift. RHIC91 has intentionally the feature to create a long drift (about 40 m) between Q4 and Q3. But if fails the use and the purpose of this drift. Despite the length of this drift, the solution so far proposed still required going through a sequence of several magnets. I have abandoned then the idea of the long drift which is also in conflict with the requirement of a not-too-long telescope. The solution I have is sketched in Fig. 43 and requires going through only one quadrupole, Q4, which is of the type #3, that is of large aperture. A vertical kicker (VK) is located between Q4 and BC3 which provides a kick angle of 4.7 mrad and it is followed by a vertical septum magnet which bends 14.3 mrad more. The scheme I propose requires a healthy kicker but a rather reasonable septum magnet.

Probably the reader has already noticed that I am violating one of my conditions: the vertical kicker should have been followed by an horizontally bending Lambertson. I have chosen a vertical kicker because its deflecting action is helped by the defocusing effect of Q4 in the vertical plane. I continue with a vertical septum magnet because I have already an offset of 7 cm at the front end and an angle of 7 mrad, and also because it is easier to clear Q5 downstream vertically than horizontally.

The beam displacement in the extraction channel is shown also in Fig. 43. At the front end of Q5 it reaches 25 cm which is required for clearing it. The location of the aborted beam with respect to Q5 is shown in Fig. 44. In Fig. 43 the beam abort is shown to occur downward, below Q5. This is preferable and could be realized by rotating Q5 upsidedown to present the shortest clearance from the beam to the outside downward. Nevertheless this requires the construction of a special cryostat where the function of the holes for refrigeration remains unchanged and only the magnet cold mass is displaced. If this is

not possible than the abort can proceed upward; once outside, the beam can be taken first horizontally away and then downward. Figure 45 shows a possible configuration of aborted and circulating beam at the front end of the vertical septum magnet. Actually this is shown here as a C-magnet surrounding the collider vacuum chamber. The acceptance to be aborted is taken to be 6 πmm·mrad but the extraction channel does not interfere with the normal acceptance of the circulating beam which is here taken to be 25 πmm·mrad matching that of the regular arcs.

The parameters of the kicker magnet and of the septum magnet are given in Tables 8 and 9 respectively. If one adopts a C-shaped magnet and controls the amount of field leakage in the regular beam enclosure there is probably no need to pulse the magnet.

Table 8: Abort Kicker Magnet.

Length	10 m
Field	4 kG
Bending Radius	2100 m
Bending Angle	4.7 mrad
Risetime	1 μs
Aperture	70×70 mm^2

Table 9: Vertical Septum Magnet for Abort.

Length	12 m
Field	1 T
Bending Radius	840 m
Bending Angle	14.3 mrad

I am the first one to notice that the kicker strength is very large (but not impossible). There are several ways one can reduce the kicker field. For instance adding a 3 m long section between BC3 and Q3 could lower the field to 3 kG. A better way is to shift Q5 closer to the regular dipole nearby. To restore the telescope properties also Q4 will move;

but in any case there will be more space that can be used by either the kicker or the septum magnet.

15. Conclusion

After all it has been said in this report I do not see the need or the case to provide a conclusion. I certainly like to urge the reader to consider my recommendations and suggestions. I would like only to point out that the only negative spot with RHICAGR is the exclusion of common quadrupoles to increase the performance of collision of beams of equal species. This choice should be pondered very carefully before the decision is made. There may be other alternatives, like stochastic cooling or the shortening of the interaction region. After all the project is going to take such a long time before it can be exploited that one may consider usage of common quadrupoles only in a distant future. In the meantime I propose to start with a lattice that I can easily commission and operate as soon as it becomes available.

ARC BISECTOR

ONE SUPERPERIOD

239.65 m   381.23 m

BLUE   RING

YELLOW

INNER ARC   INSERTION

2 x 141.75 m

X-ING POINT

OUTER
ARC

X   Y - LINE

INJECTION
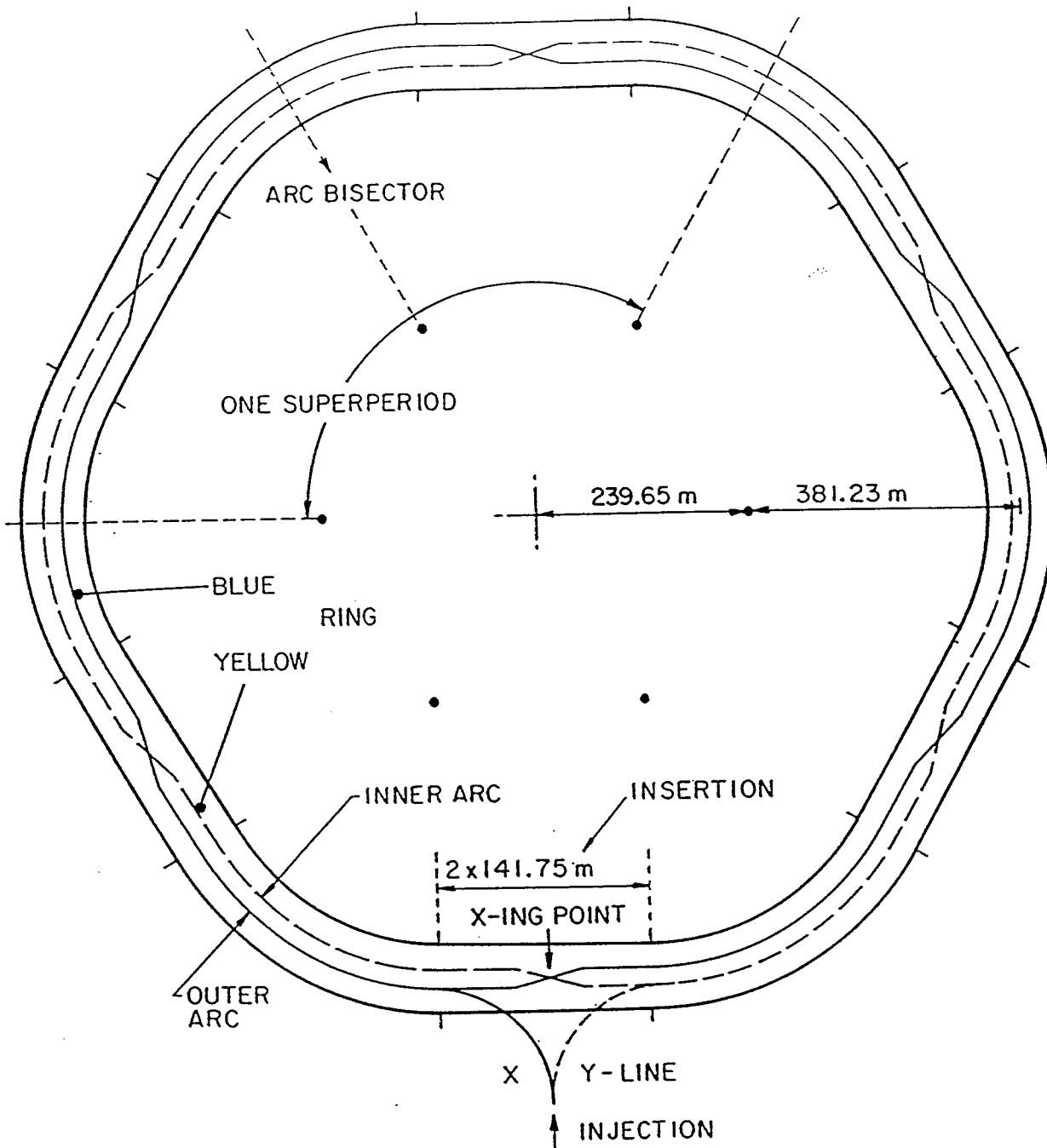
Fig. 1   Layout of the Collider.

Regular Arc Cell

$B\rho = 839.5 \; T \cdot m$

QF

B

QD
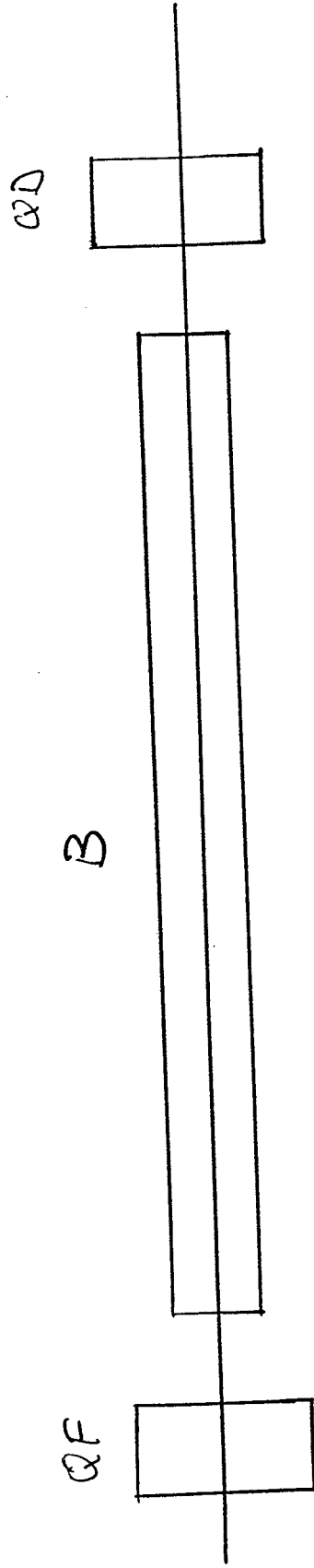
QF, QD	1.13 m	80 mm bore
	9.45 m	80 mm bore
B	75 T/m	
	3.32 T	
D	outer	2.1239 m
	inner	2.1071 m
	average	2.1155 m
Bending Radius	ρ = 253.1137 m	
Bending Angle	θ = 37.335 mrad	

Fig. 2   Regular Arc Cell (RHICAGR).

Fig. 3   Half Long Straight Section   (RHICAGR).

B   QF   QD   B2   B2   QD(K)   B   Q5   Q4   BC3   Q3 Q2 Q1   BC2 BC1   type

QD   QF   QD   QF   QF   QF   x

1   1   1   1   1   (2) 1   1   3   2   3 2

Arc   Dispersion Killer   Long Telescope

$\alpha = 0.$

6.6 mrad

9.8 m →

BC1

7.0 m

1.3090 m

1.7886 m

↓ BC2

↓ Q1

Q2

189 mm

Q3

4.1642 m

5.3092 m

BC3

450 mm

bore :   200 mm

80 mm

80 mm

θ_1 = 18.836 mrad

θ_2 = 5.382 mrad

θ_3 = 13.454 mrad

BC1 :   3.7 m

BC2 :   1.3622 m

BC3 :   3.4054 m

ρ (BC1)   = 196.4348 m

ρ (BC2 & BC3) = 253.1137 m

B = 4.274 T

= 3.317 T

Fig. 4   Beam Crossing Scheme in RHICAGR.

Fig. 5   A Short-Telescope Solution for RHICAGR.

Fig. 6   The Layout of RHIC91.
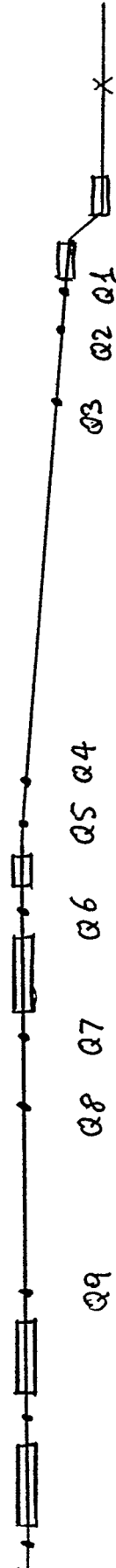
Dispersion, X_p
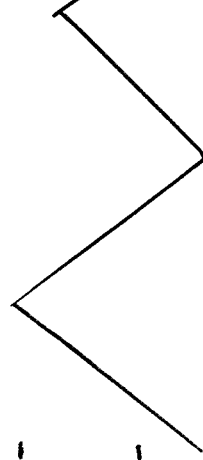
Fig. 7   The Dispersion in RHICAGR. $\beta^* = 2m.$

43
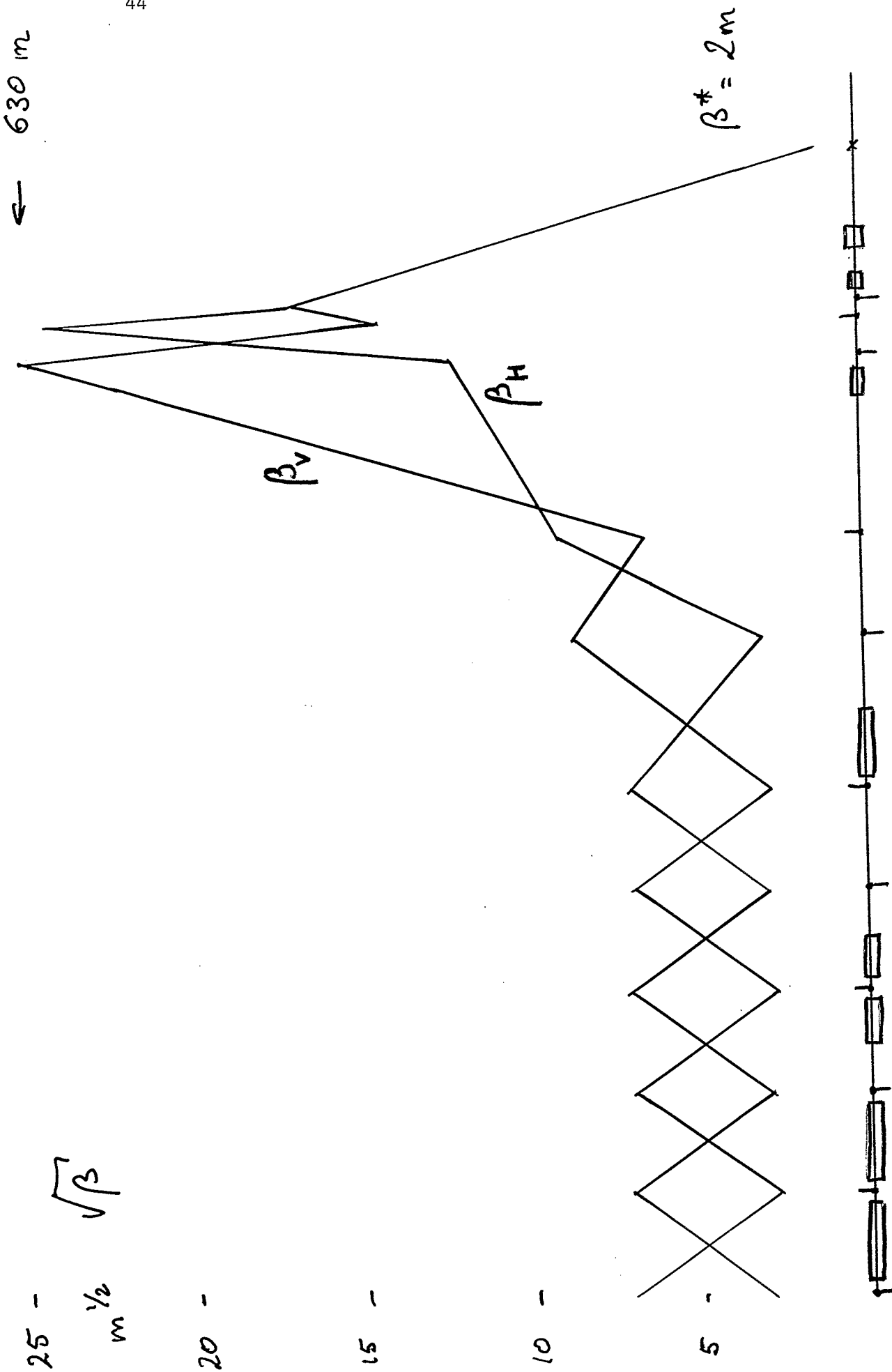
Fig. 8   The β-Functions in RHICAGR.
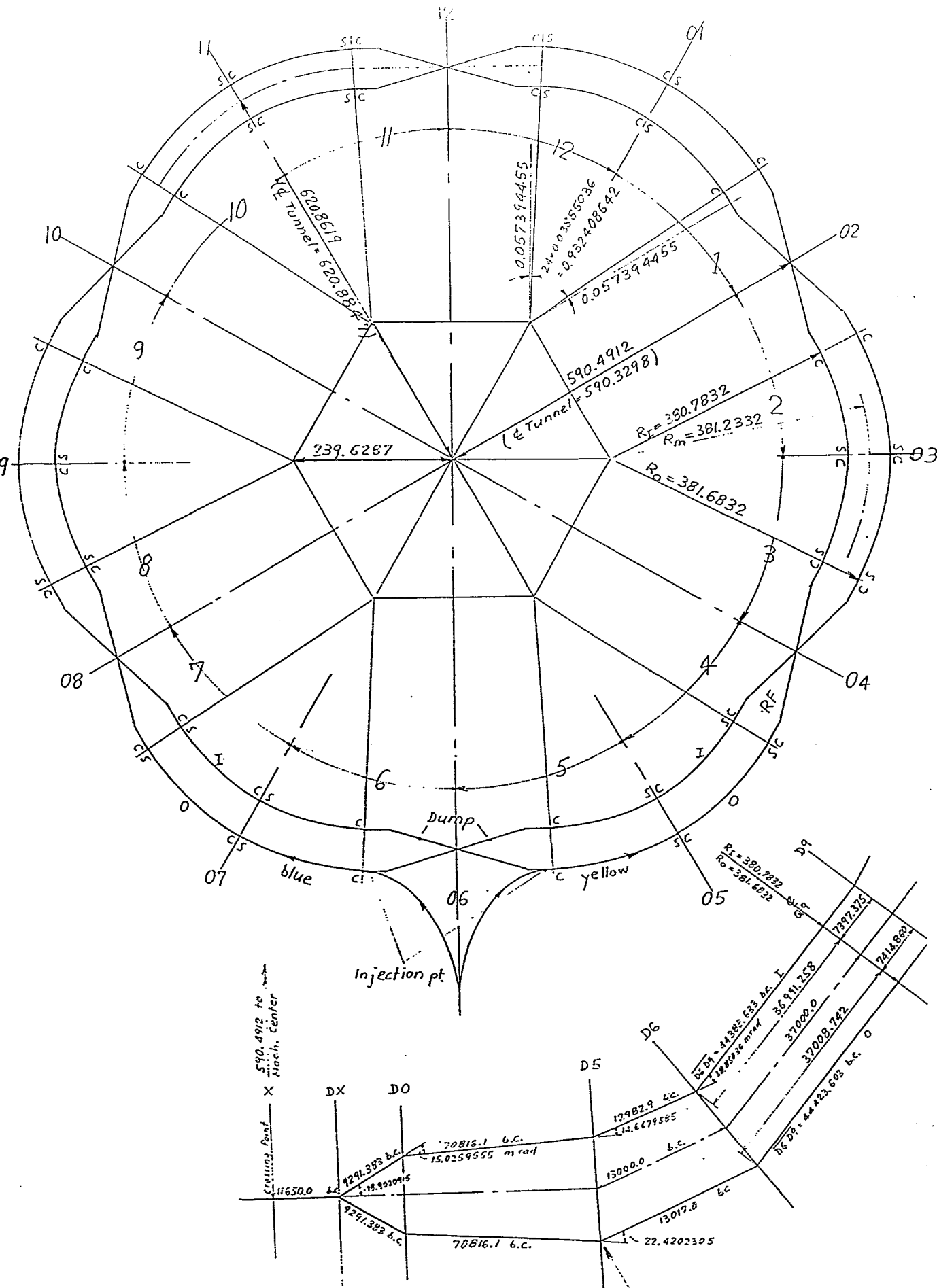
Fig. 9 RHIC Machine Geometry July 91

46

MAGNET / CRYOSTAT ASSEMBLY

171.28 cm

90.00 cm

43.00 cm

0 Sextant Center

R249.40 cm

127.00 cm

89.06 cm

100.00 CM

CENTER OF RING

Fig. 10   Location of RHICAGR at the End of Arcs.
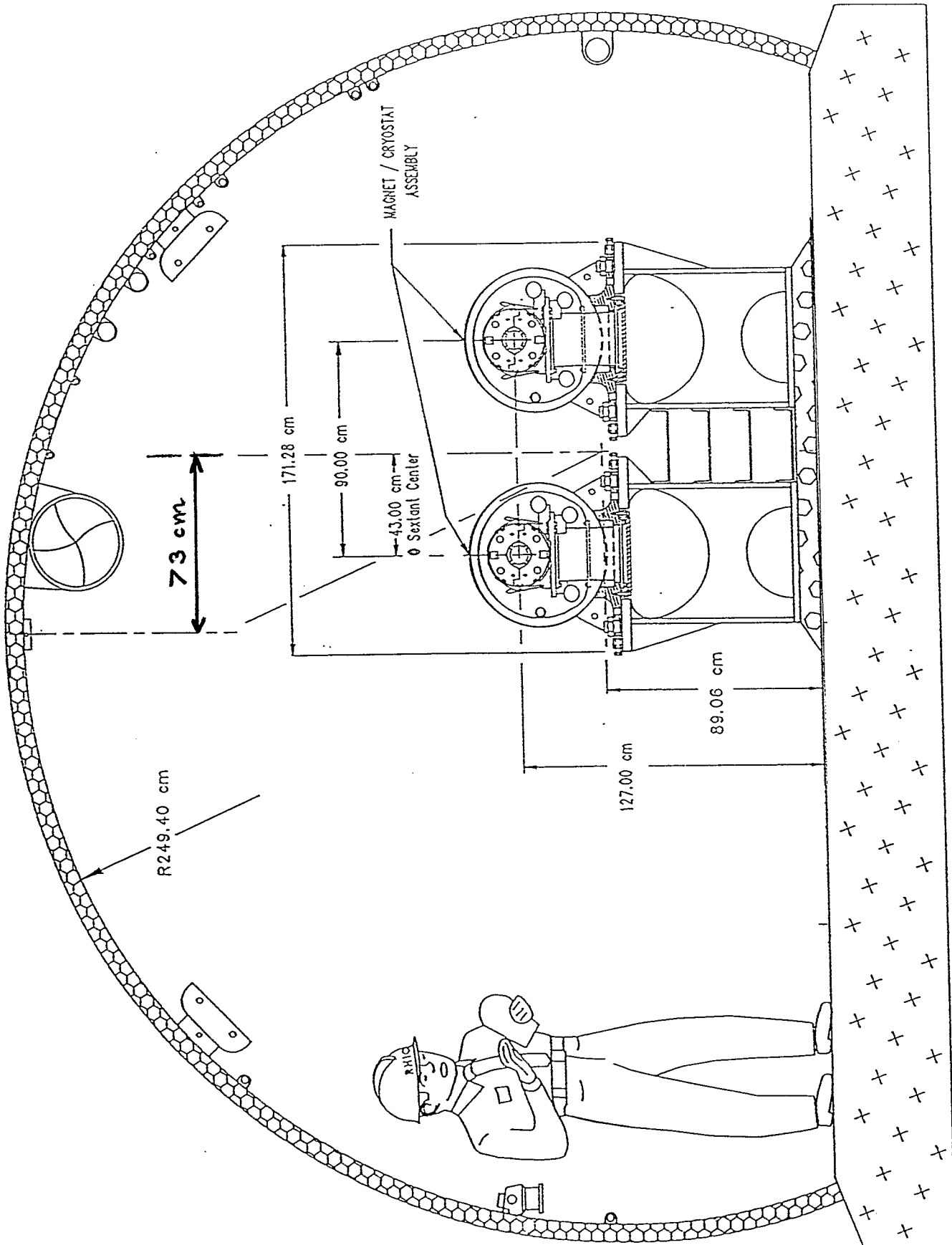
CENTER OF RING

NOTES:
1. THE LOCATION OF MAGNETS, WITH RESPECT TO TUNNEL CENTERLINE, VARIES IN ACCORDANCE WITH LATTICE CALCULATIONS.

Fig. 11   Location of RHICAGR in the Middle of Arcs.
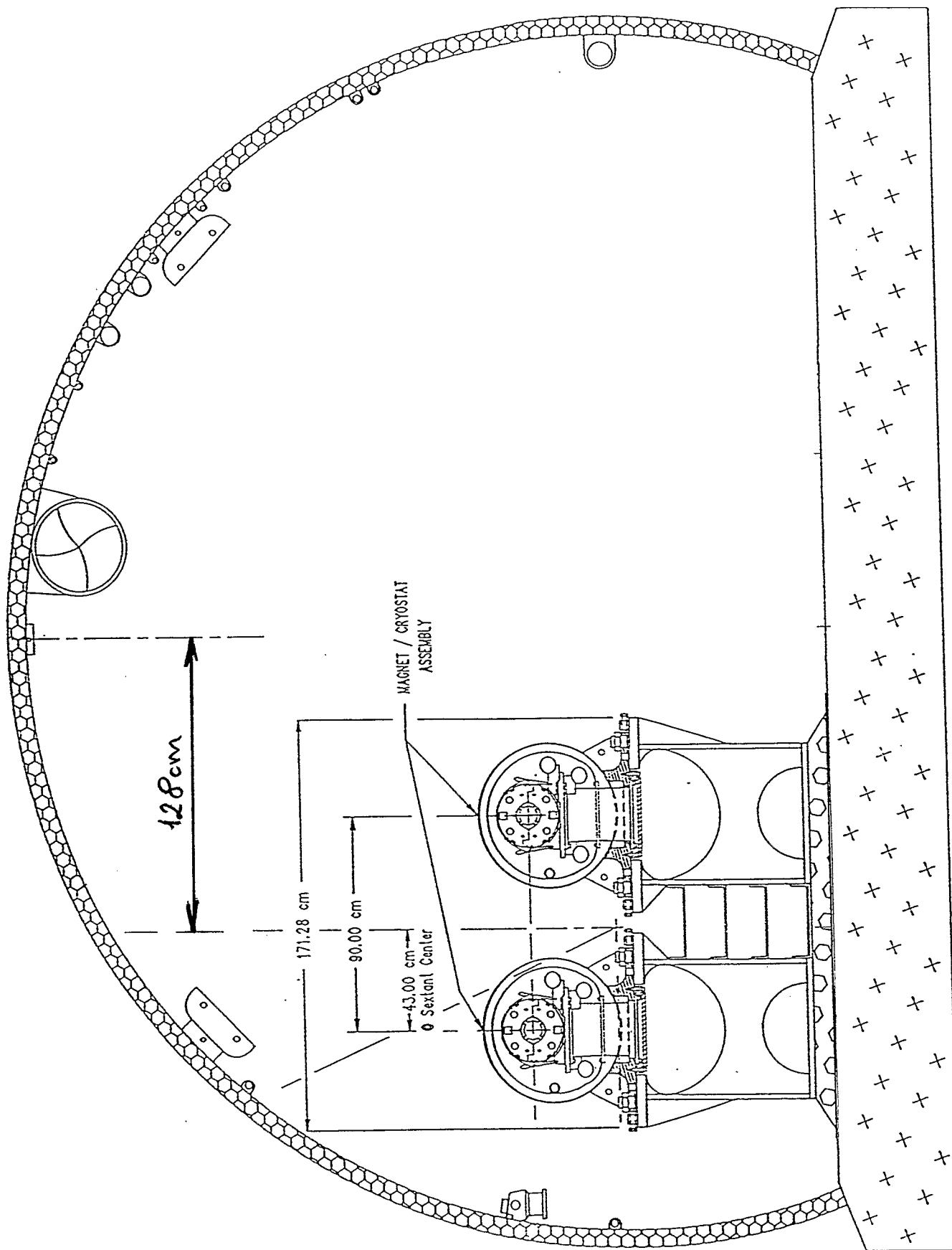
48

NOTES:

1. THE LOCATION OF MAGNETS, WITH RESPECT TO TUNNEL CENTERLINE, VARIES IN ACCORDANCE WITH LATTICE CALCULATIONS.

CENTER OF RING

MAGNET / CRYOSTAT ASSEMBLY

128cm

171.28 cm

90.00 cm

43.00 cm
Ø Sextant Center

100.00 CM

Fig. 12   Location of RHICAGR at the Crossing Point.

X_p in m

2.0

1.0
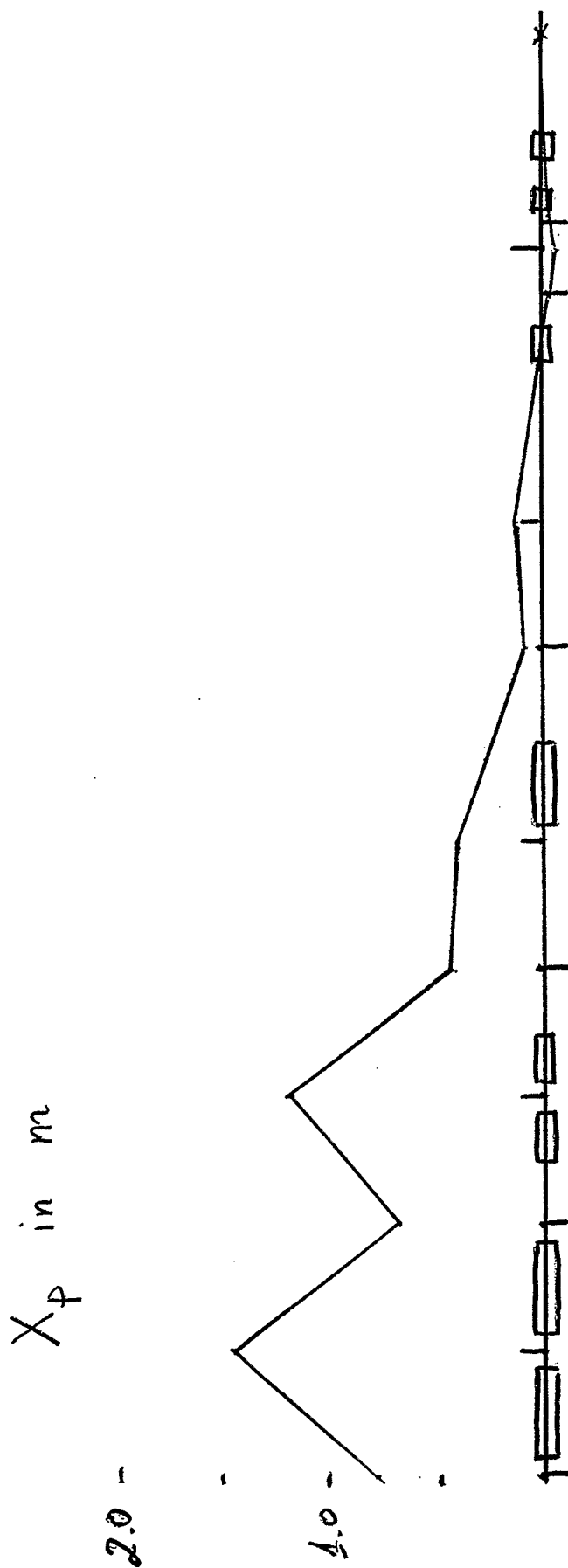
Fig. 13   Dispersion Behavior in RHICAGR for $\hat{\beta}^* = 1m$.

Fig. 14   Dispersion Behavior in RHICAGR for β^*=16m.

$\sqrt{\beta}$

1250

β_H

β_V

Fig. 15 β-Functions in RHICAGR for $\beta^*=1m.$

30

$\frac{1}{2}$

m

20

10

52
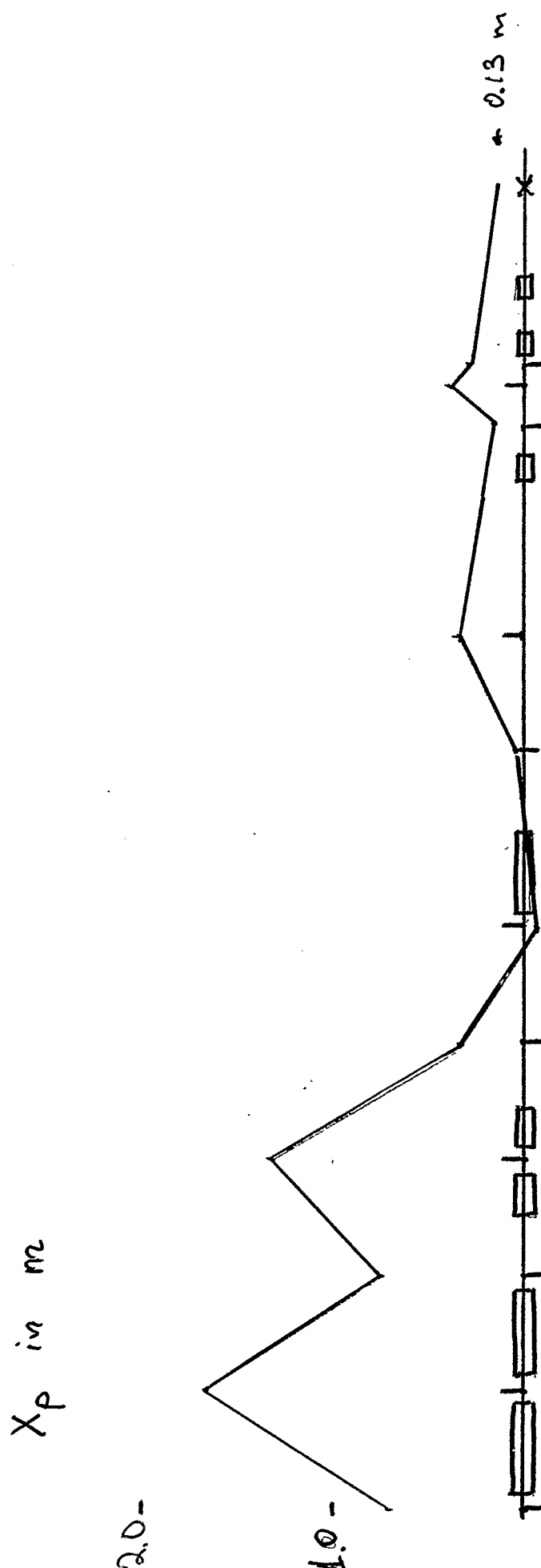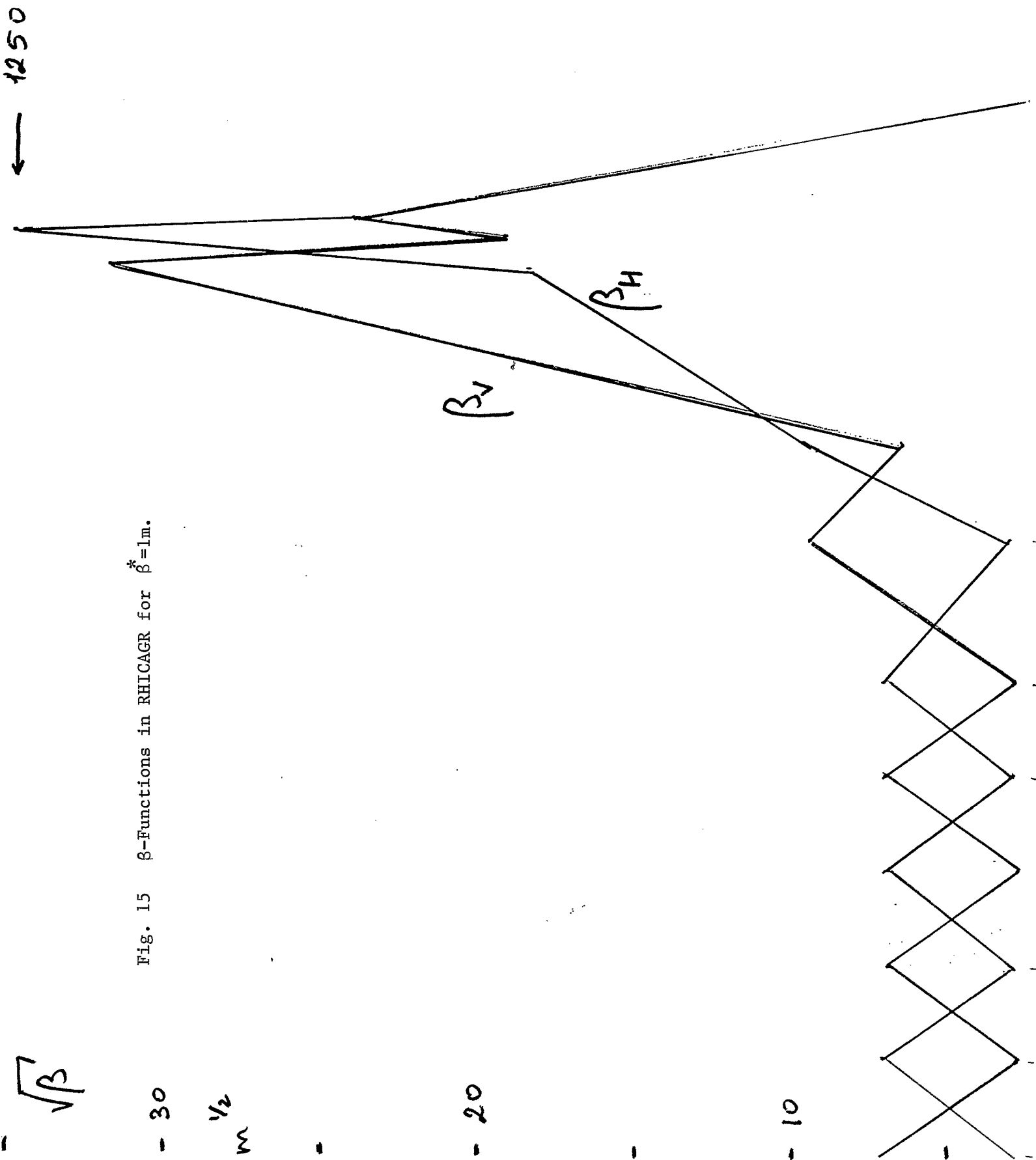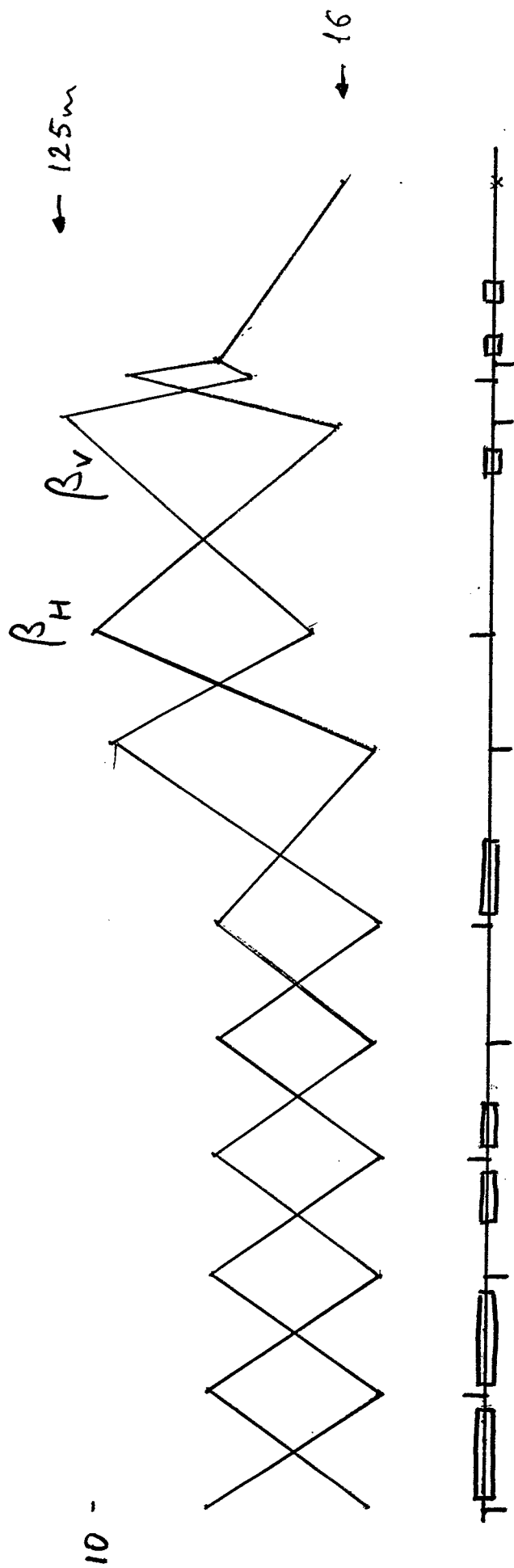
Fig. 16 β-Function in RHICAGR for $\beta^* = 16m$.

Fig. 17   Variation of Gradient in the Regular Quadrupoles   QF,QD.
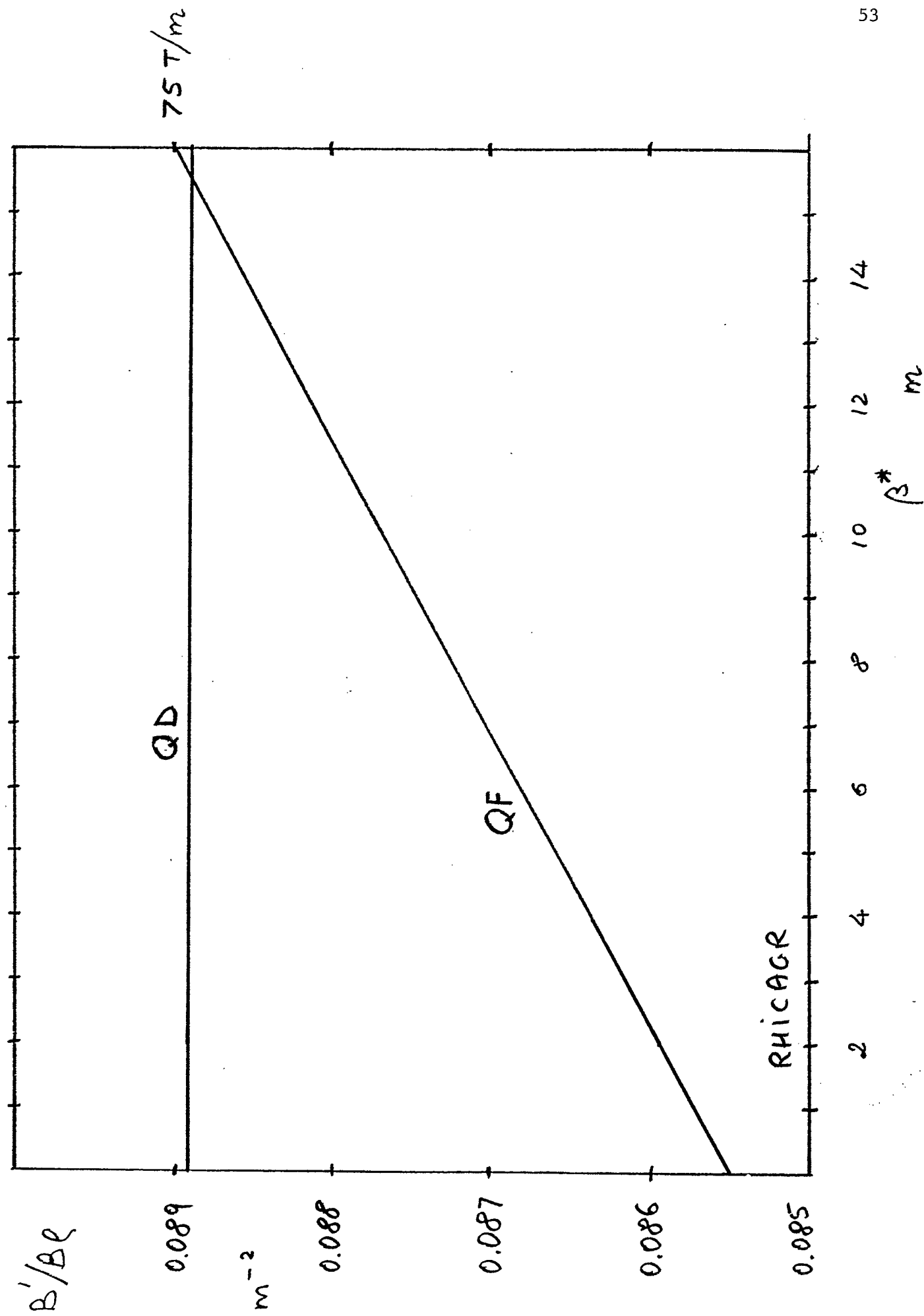
Fig. 18   Variation of Gradient in the Telescope Quadrupoles, Q1 to Q5.
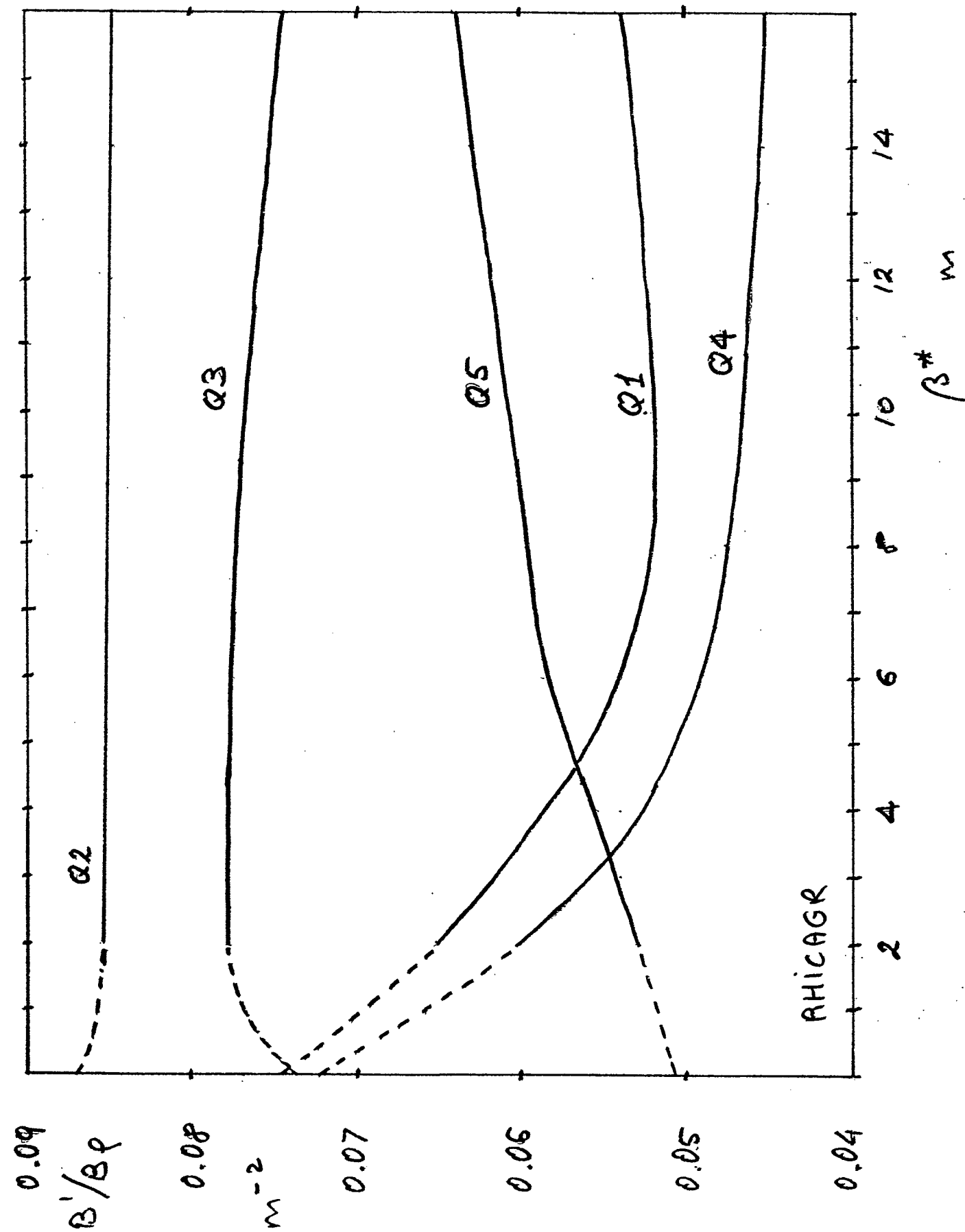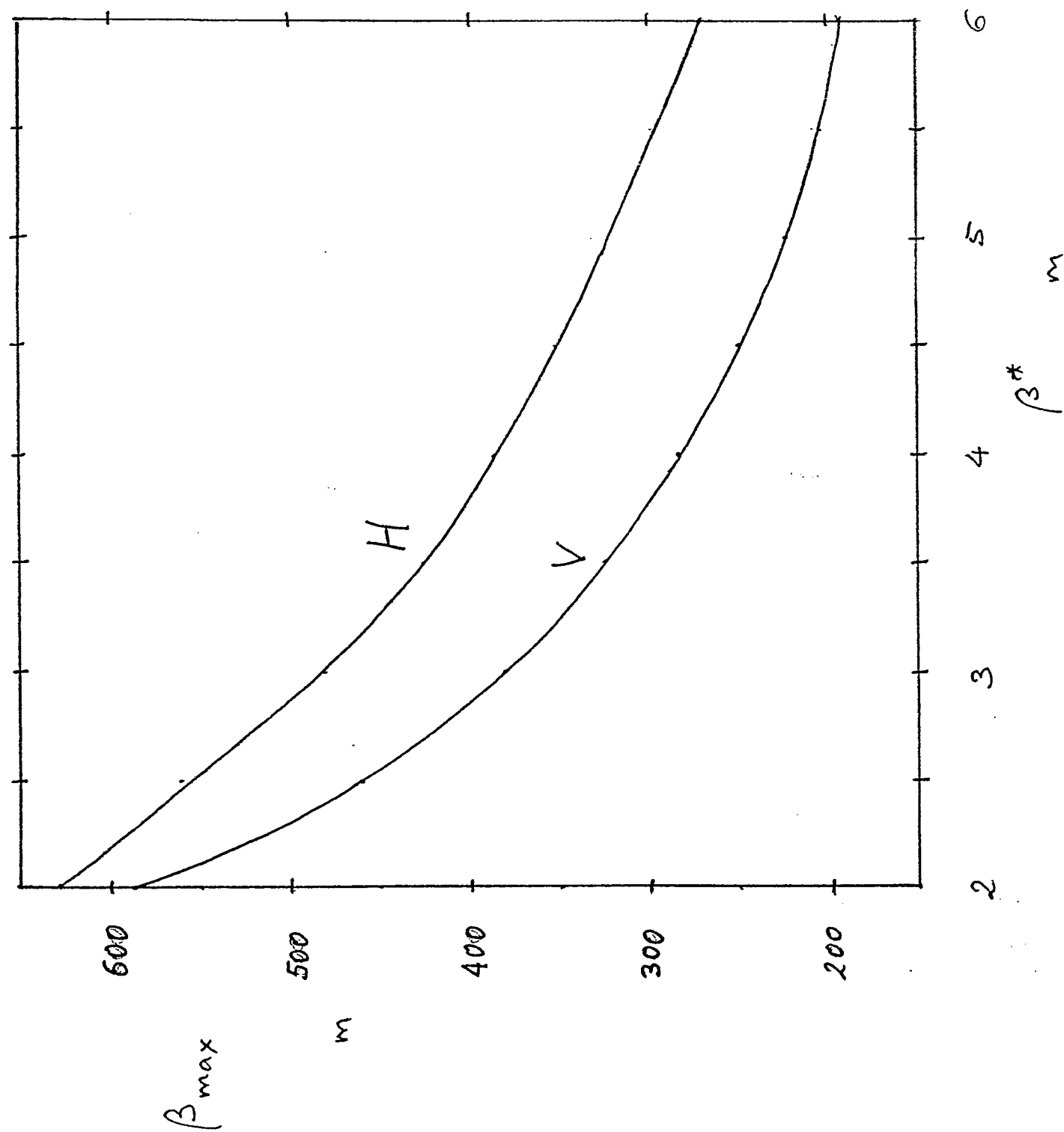
Fig. 19   Variation of Maximum β-Value in RHICAGR.
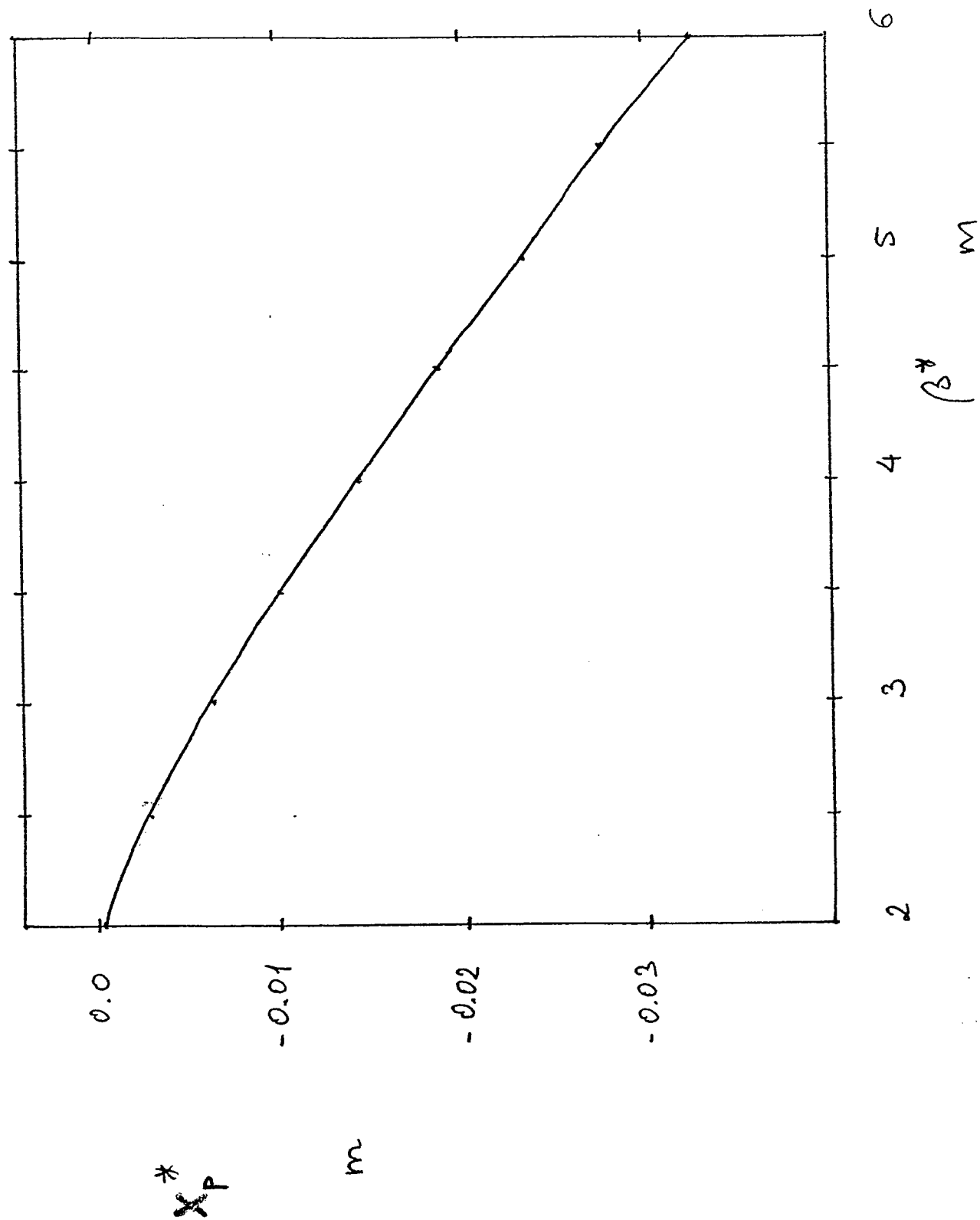
Fig. 20 Change of X_p^* with β^* in RHICAGR.
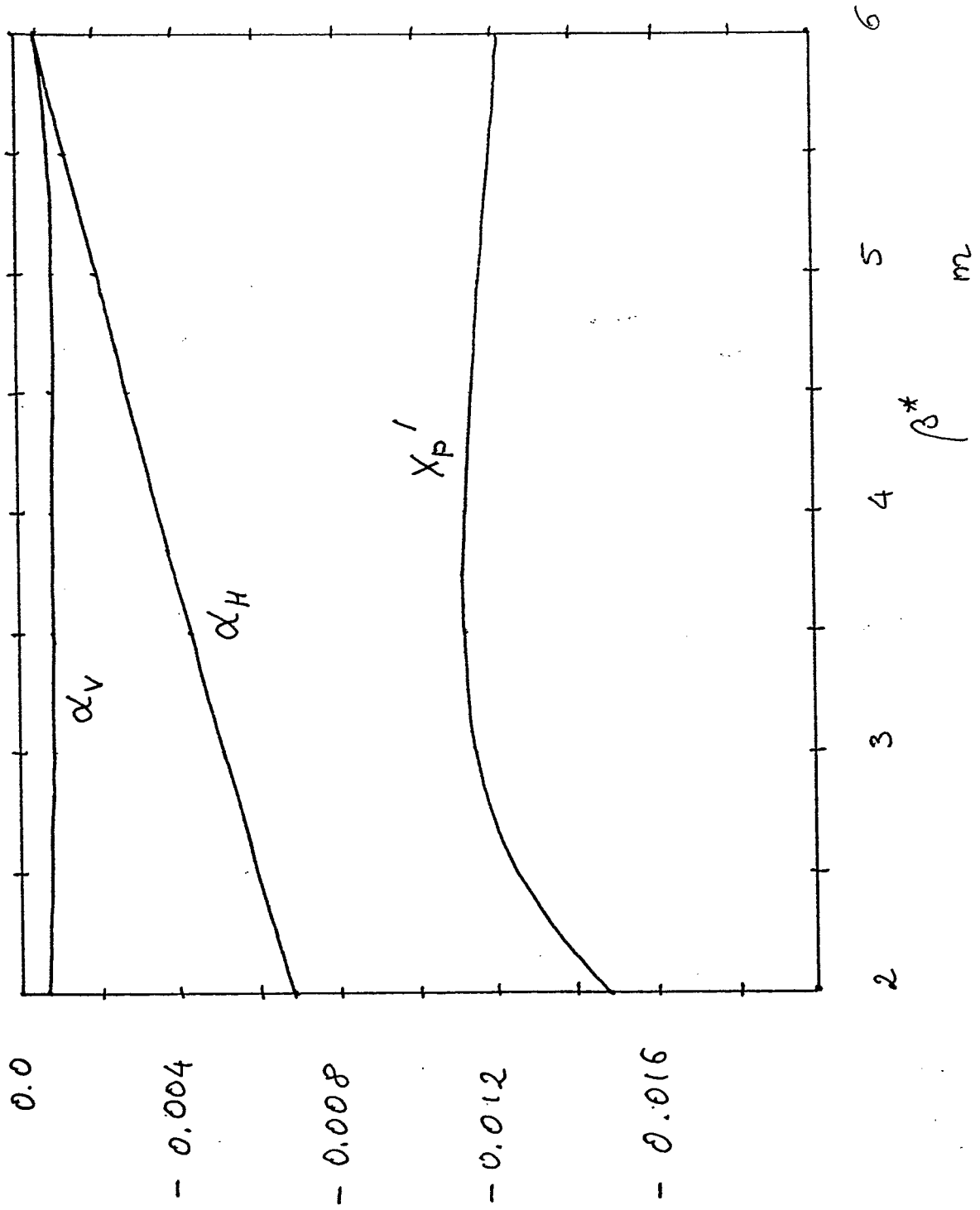
Fig. 21   Change of the Waist Parameters with β^* in RHICAGR.
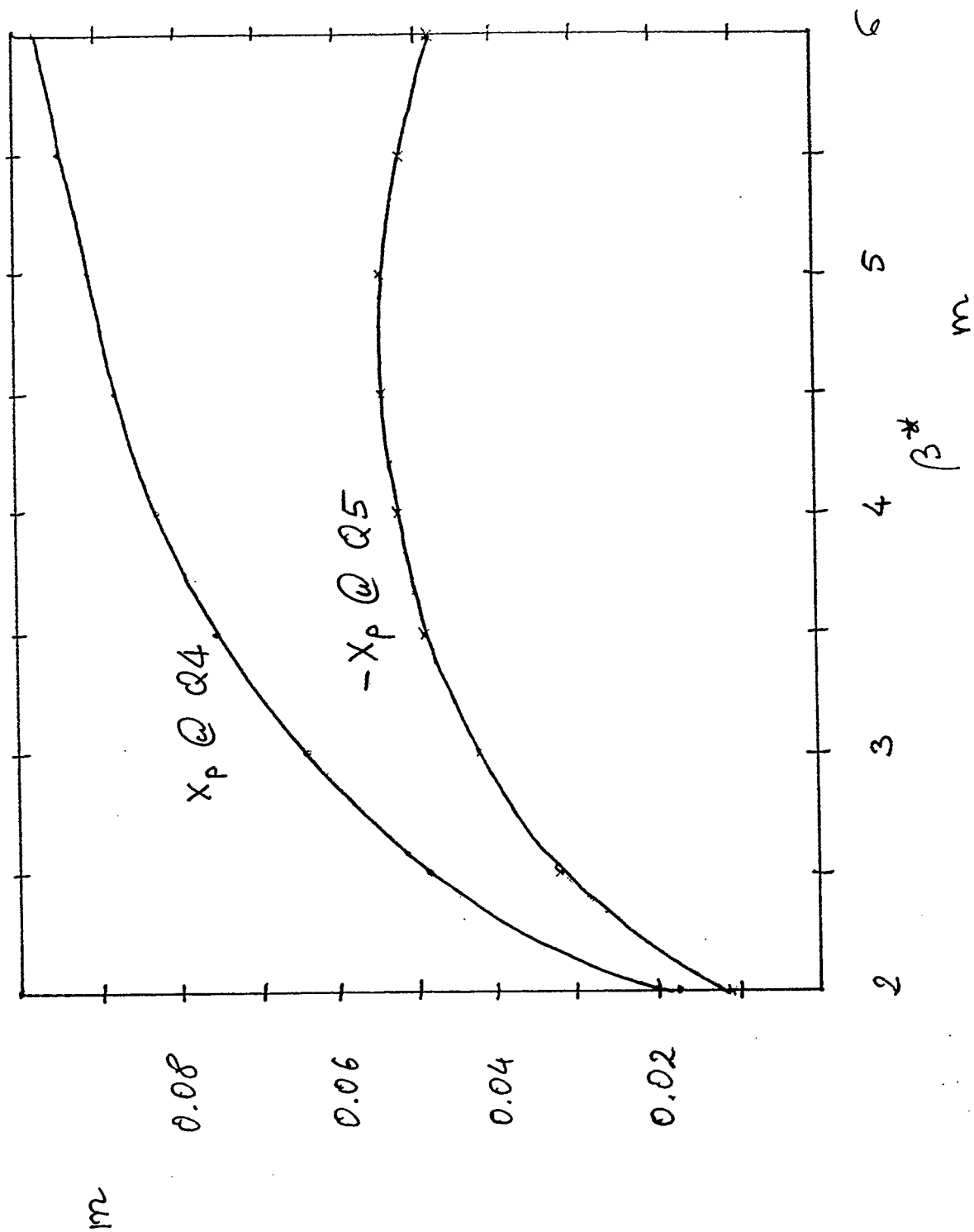
Fig. 22 Upset of Dispersion Killer During β -Squeeze in RHICAGR.
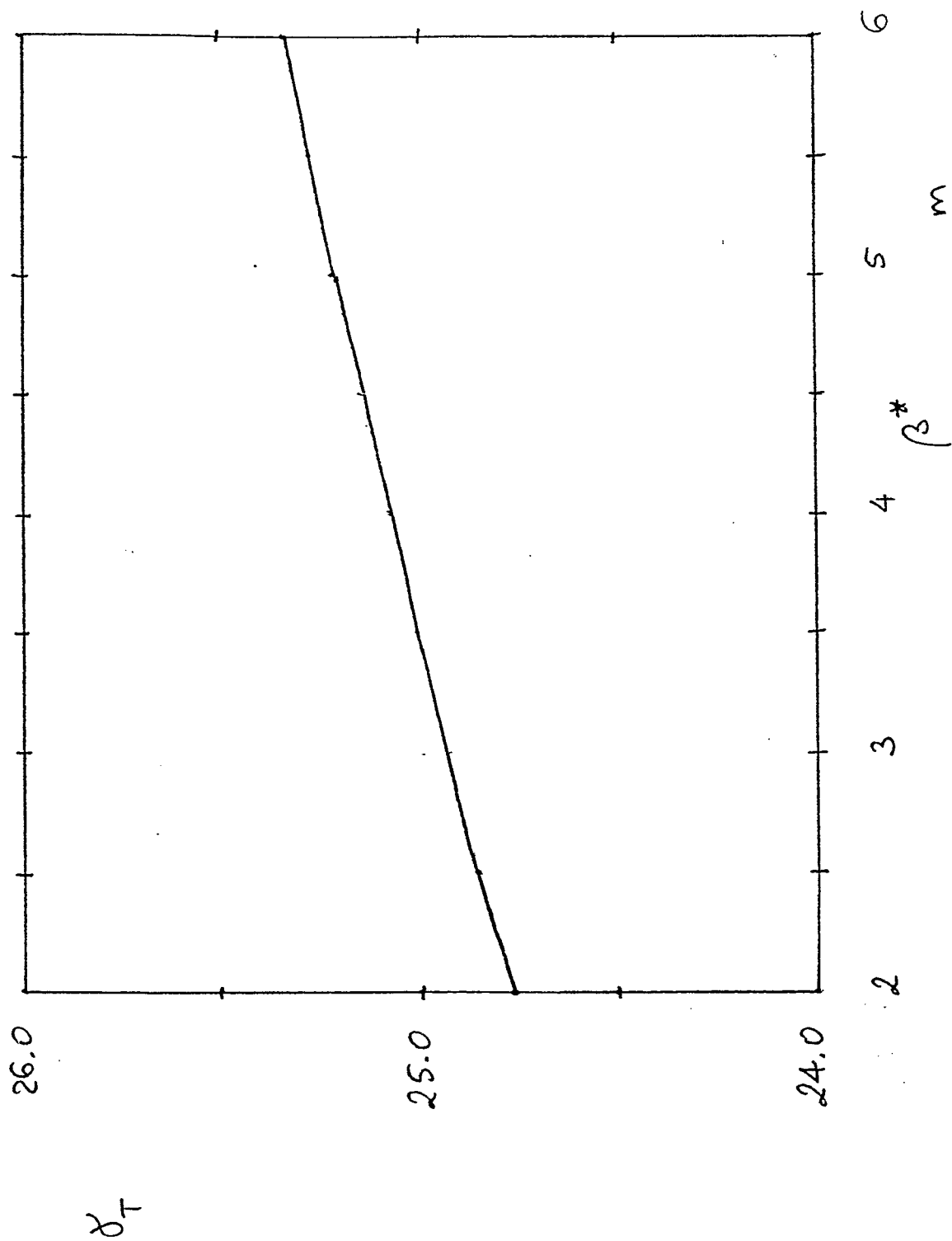
Fig. 23   Variation of the Transition Energy in RHICAGR with β^*.
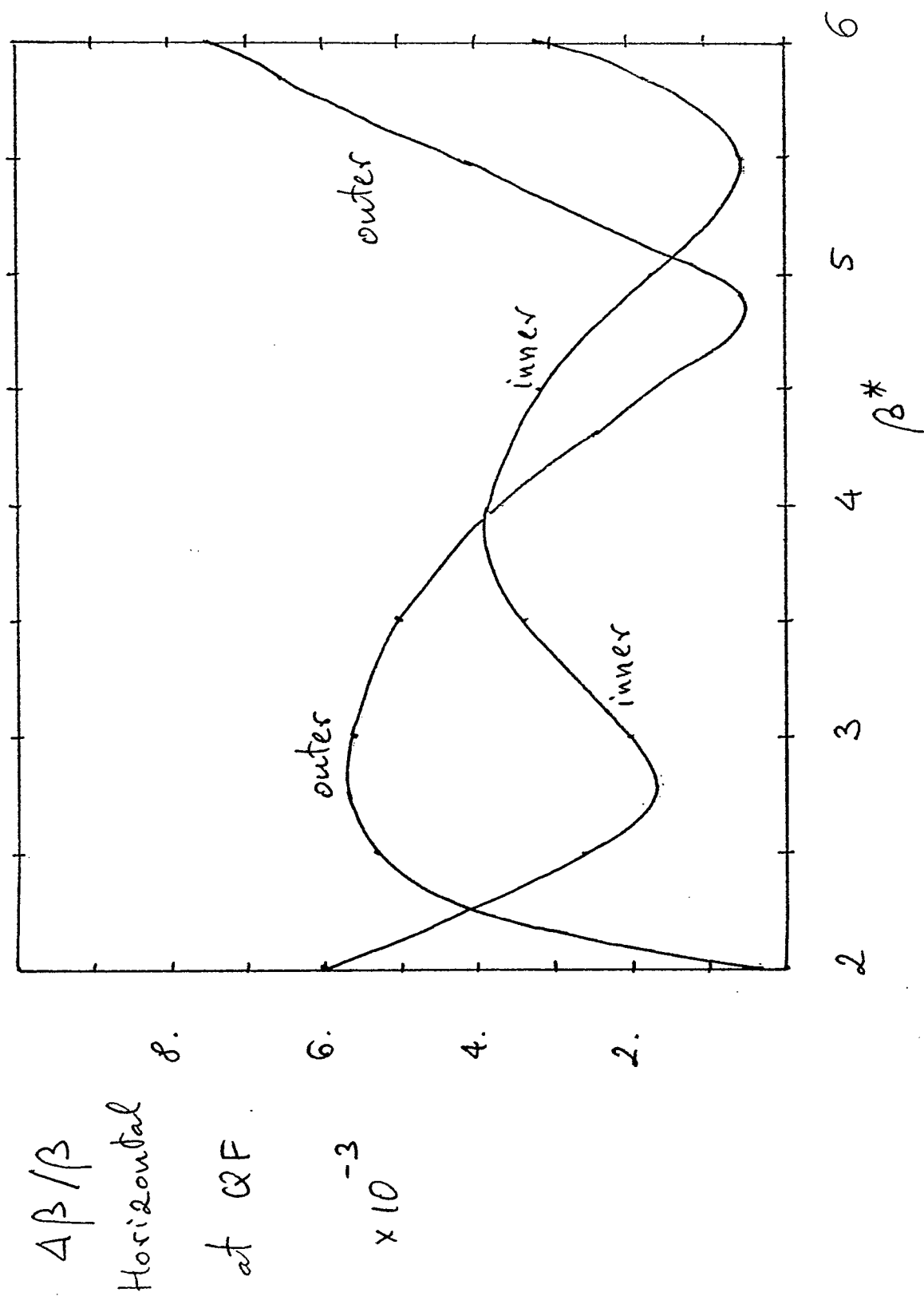
Fig. 24 Horizontal β-Distortion in RHICAGR during β-Squeeze.
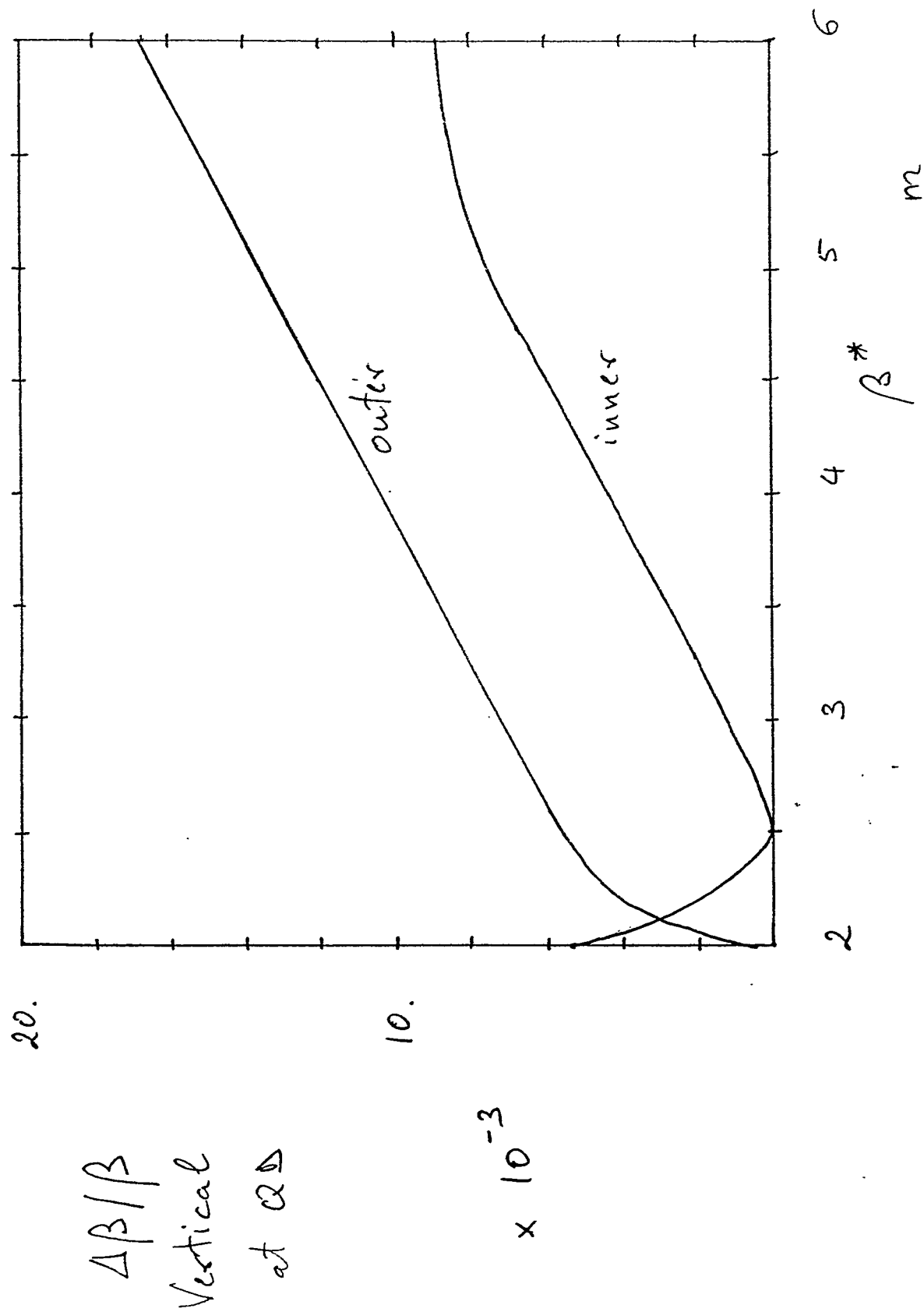
Fig. 25   Vertical β-Distortion in RHICAGR During β-Squeeze.
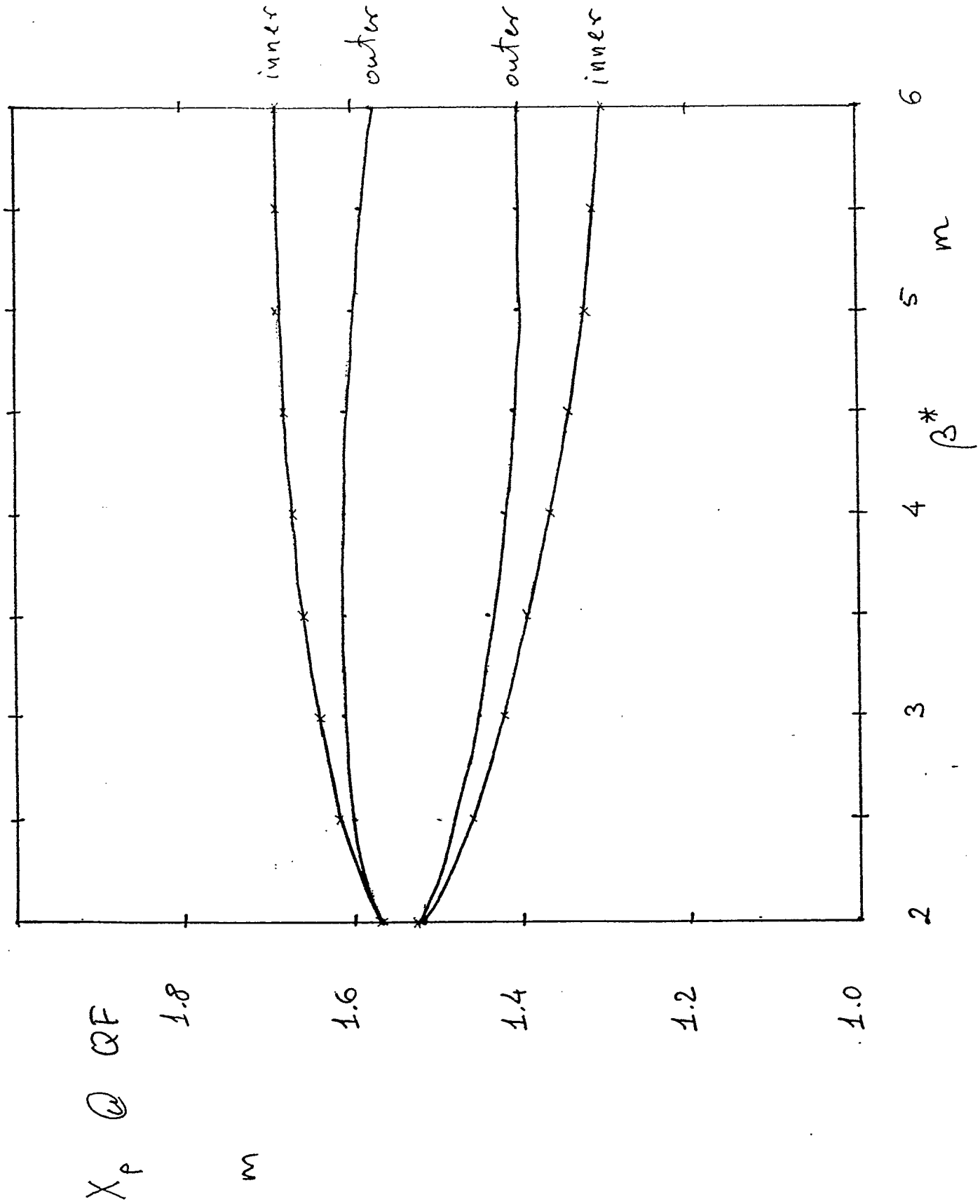
Fig. 26 Range of the Distortion of the Dispersion in RHICAGR with β^*.

Fig. 27   Betatron Tuning of RHICAGR.
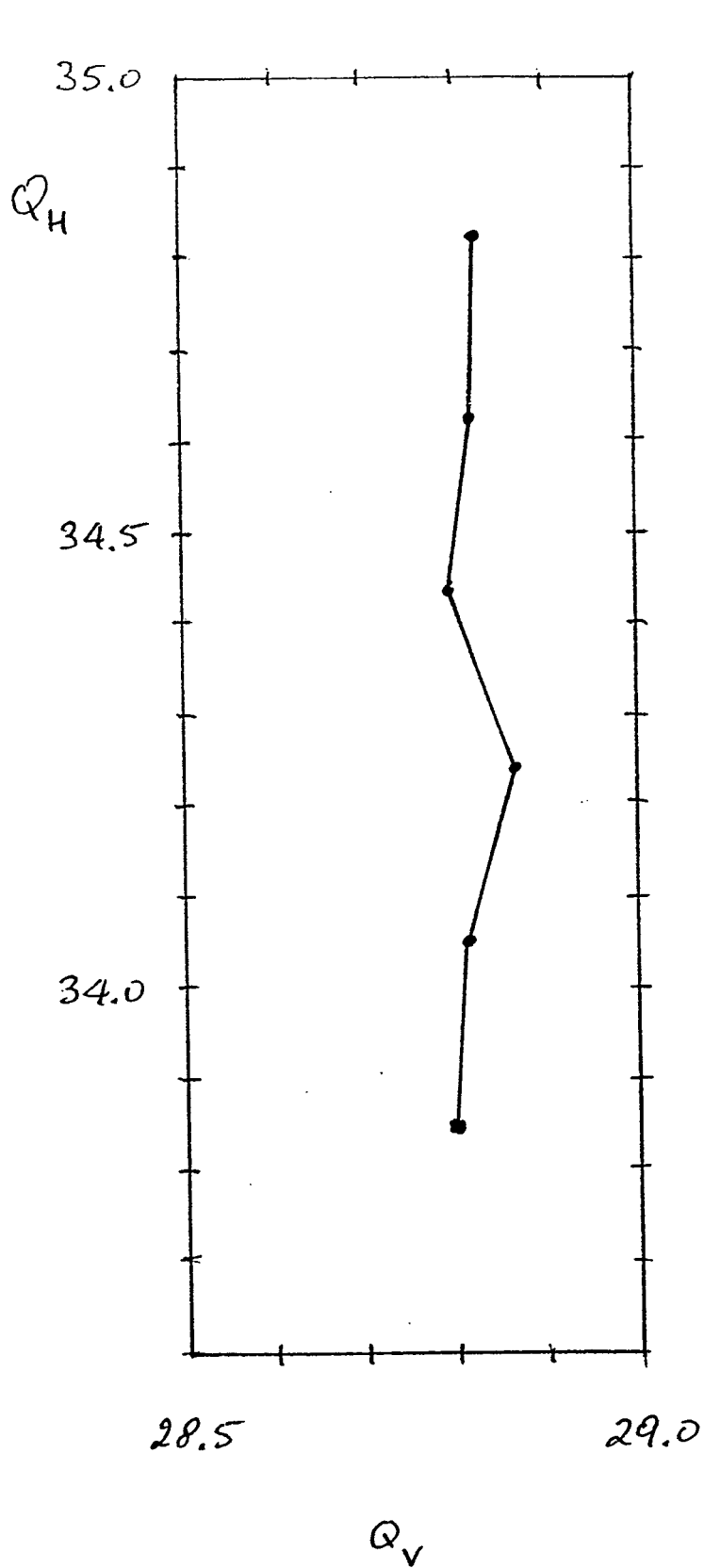
$$\beta^{*} = 2m$$

	0.08593	−0.08889
	8547	8883
	8501	8874
	8454	8868
	8406	8858
	8357	8849
	↑	↑
	QF	QD

Q_H

35.0

34.5

34.0

28.5

29.0

Q_V

$$\frac{\Delta G_F}{G_F} \approx \frac{\Delta Q_F}{Q_F}$$

Fig. 28   Variation of the Quadrupole Gradients
During Betatron Tuning in RHICAGR.
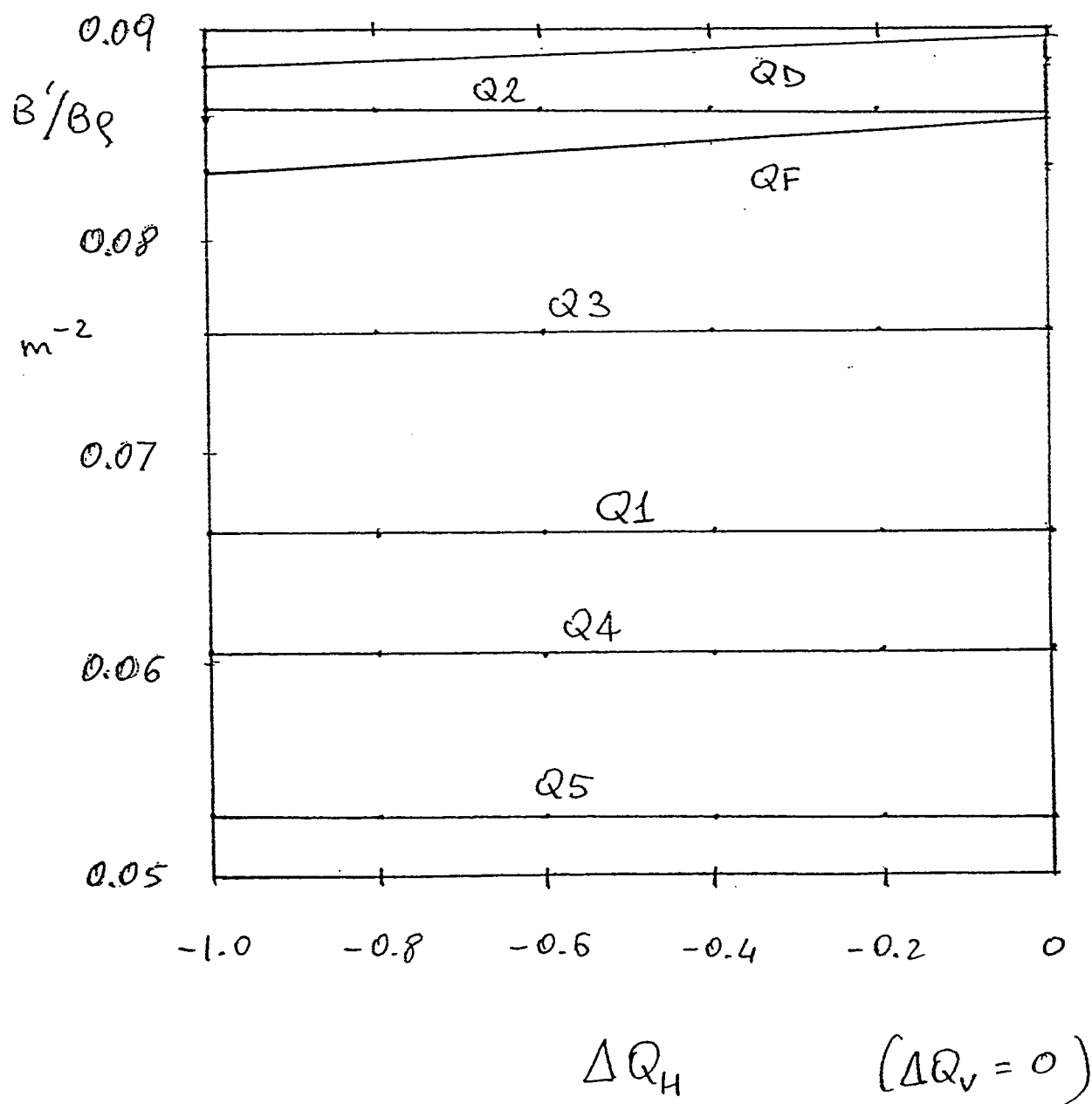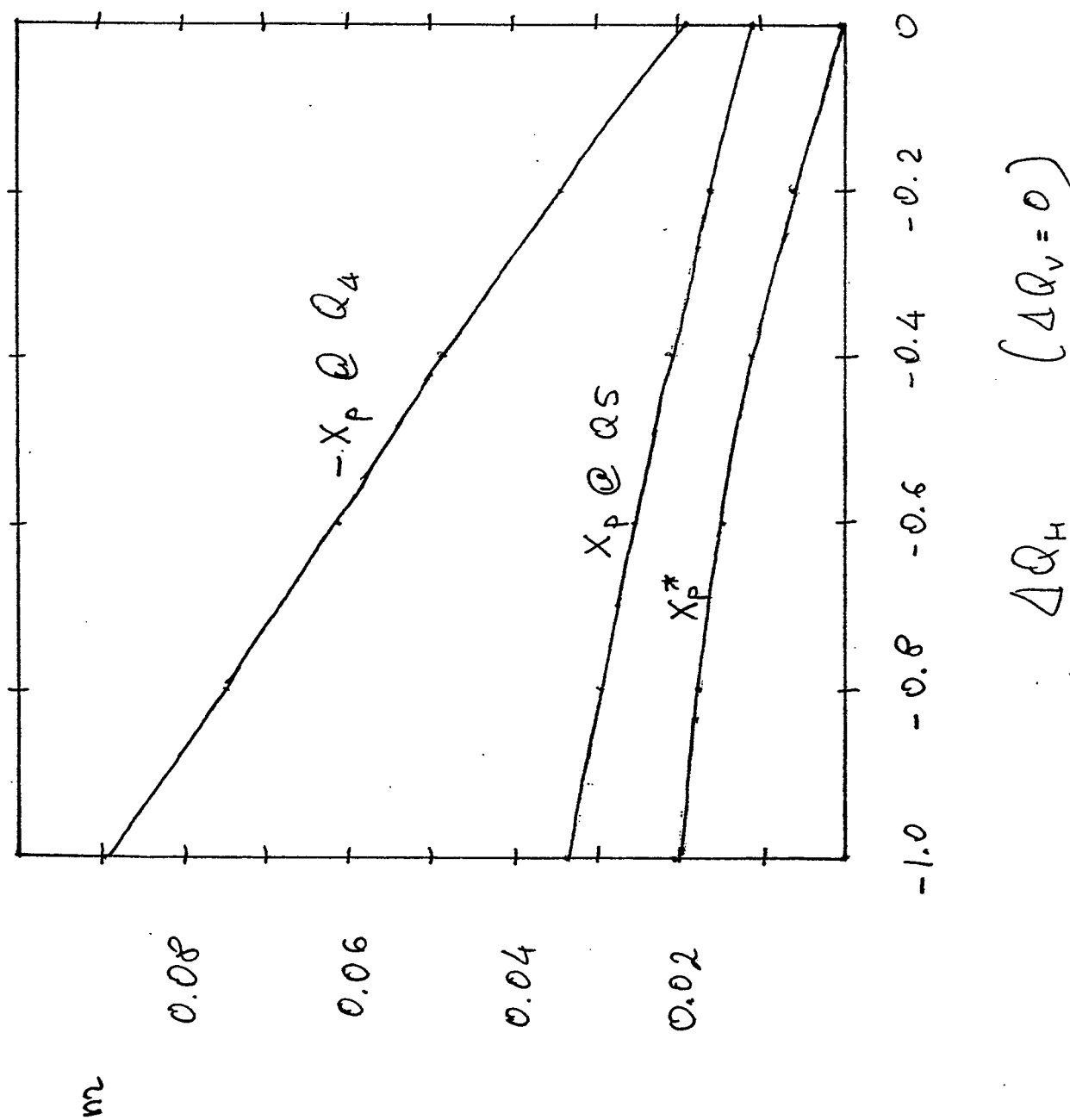
Fig. 29   Change of the Dispersion During Betatron Tuning in RHICAGR.

Fig. 30 Natural Chromaticity in RHICAGR versus β^*.
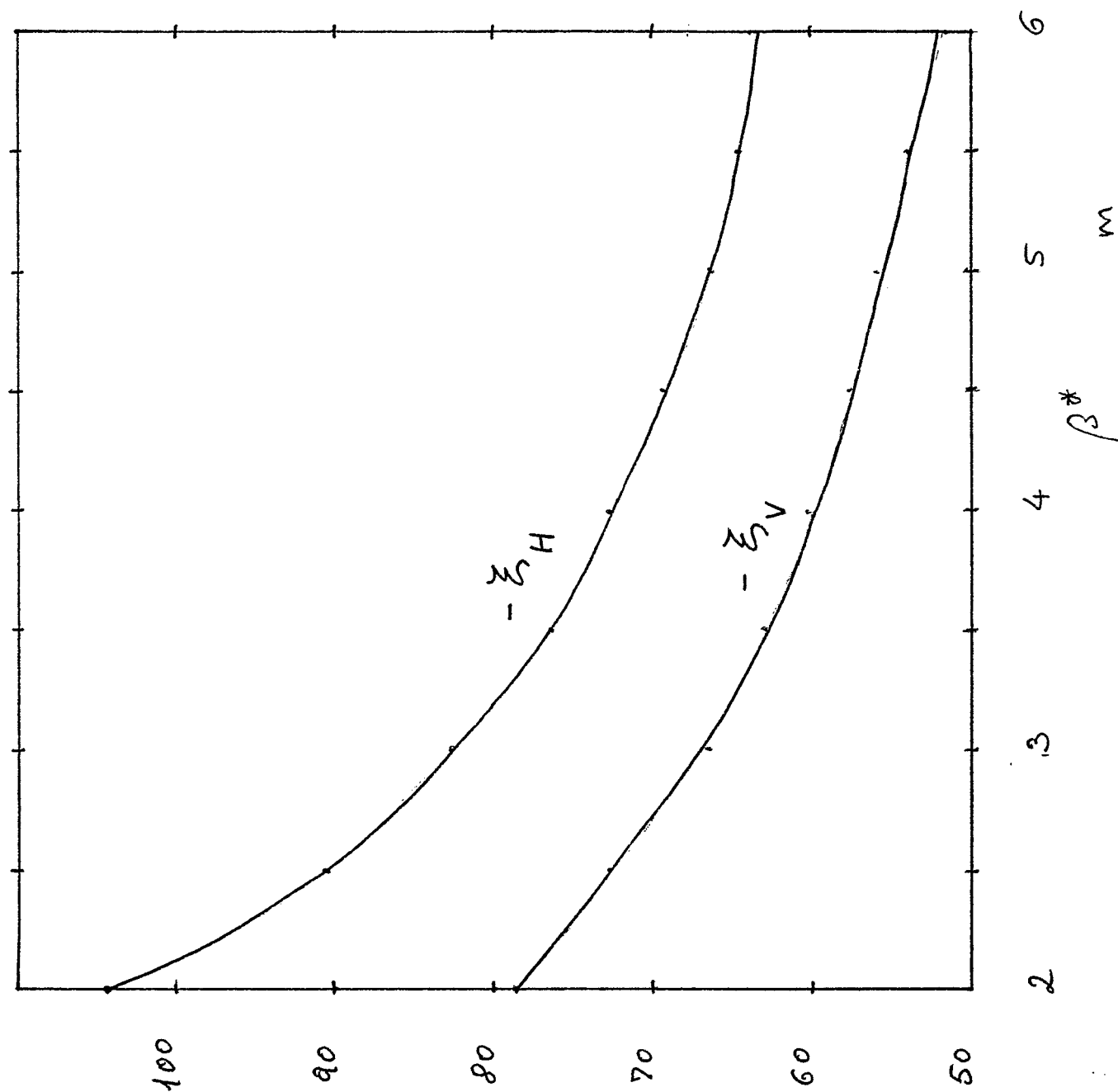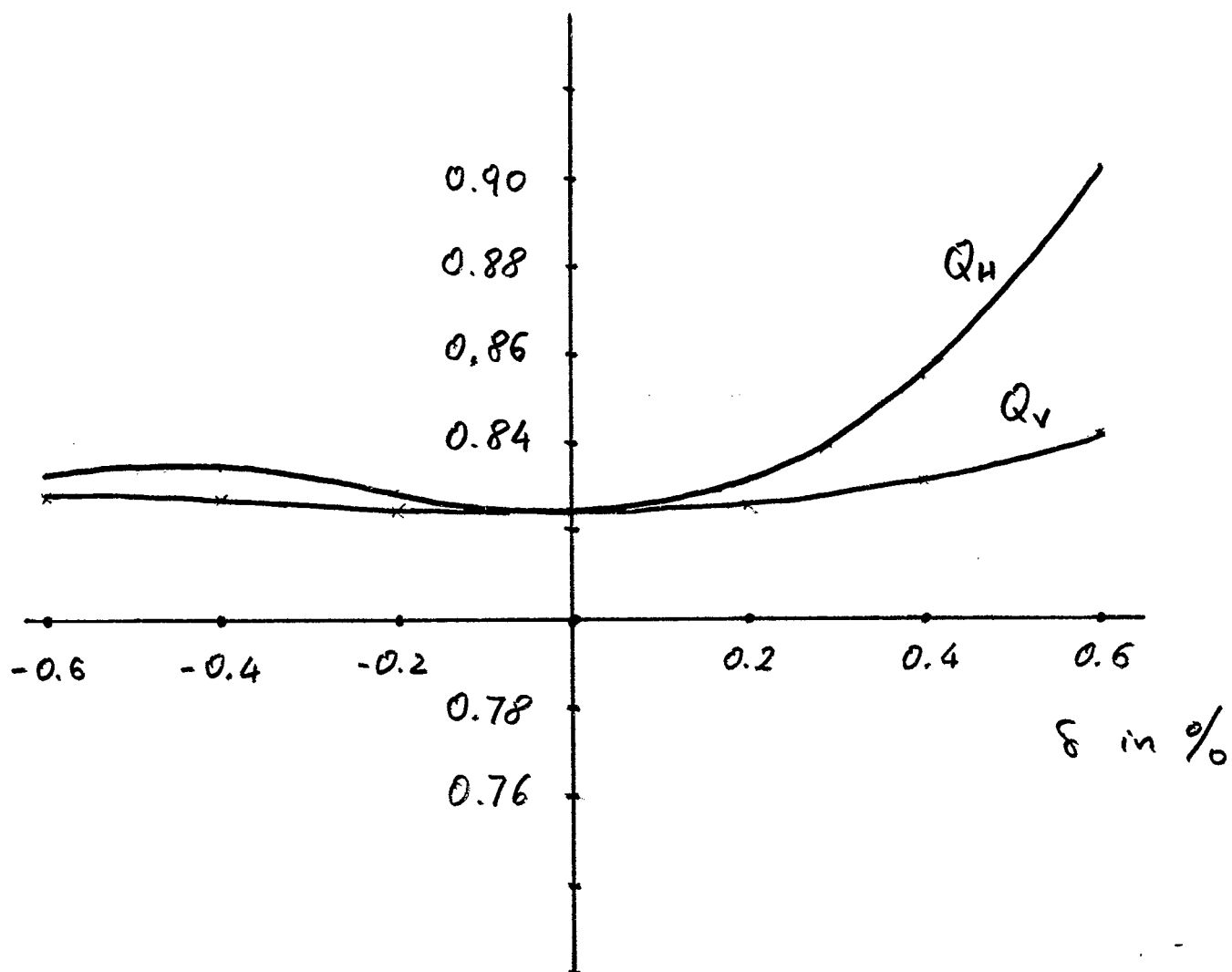
Fig. 31   Chromaticity in RHICAGR with Two
Sextupole Families.
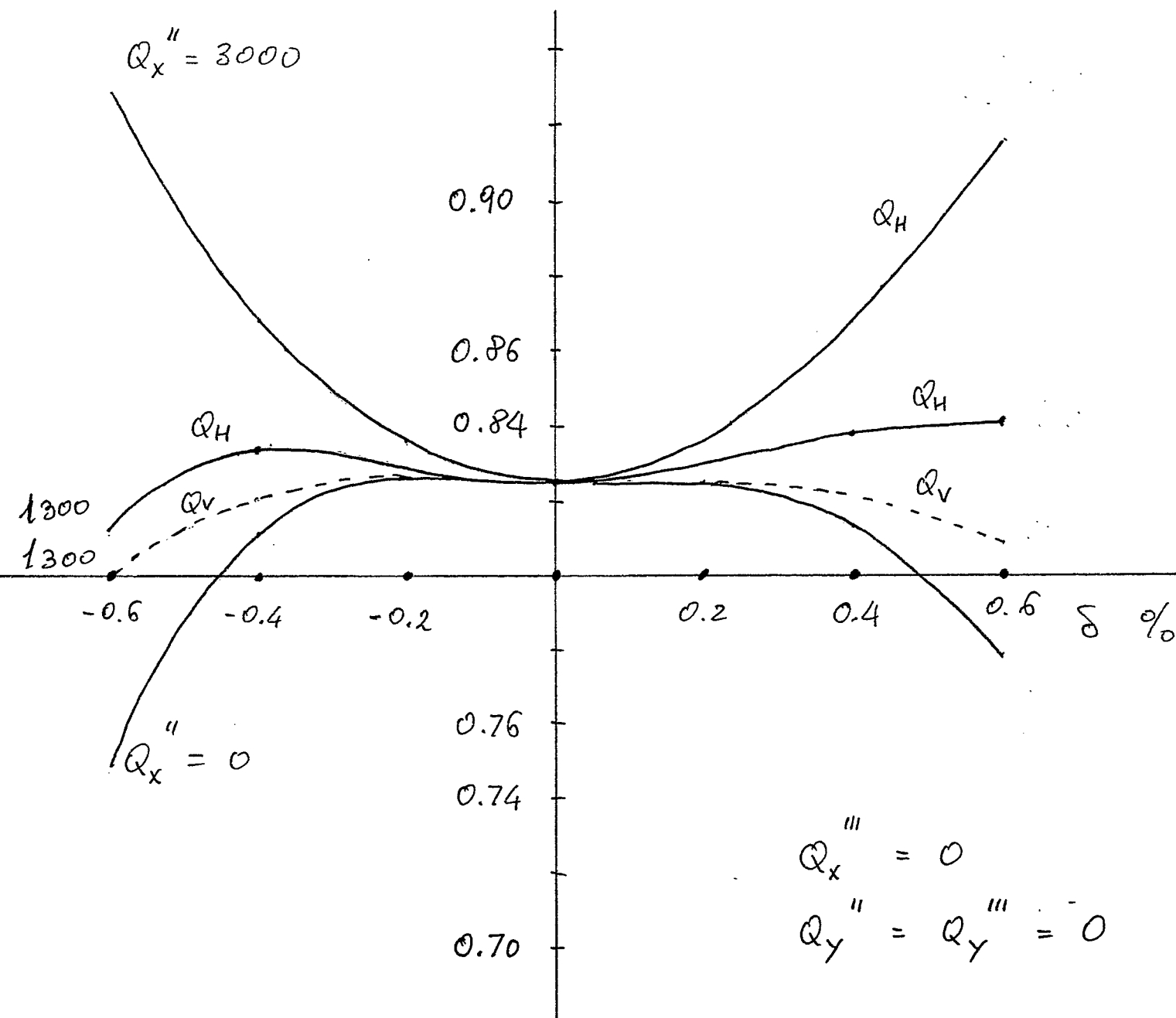
Fig. 32   Chromaticity in RHICAGR with Eight
Sextupole Families.
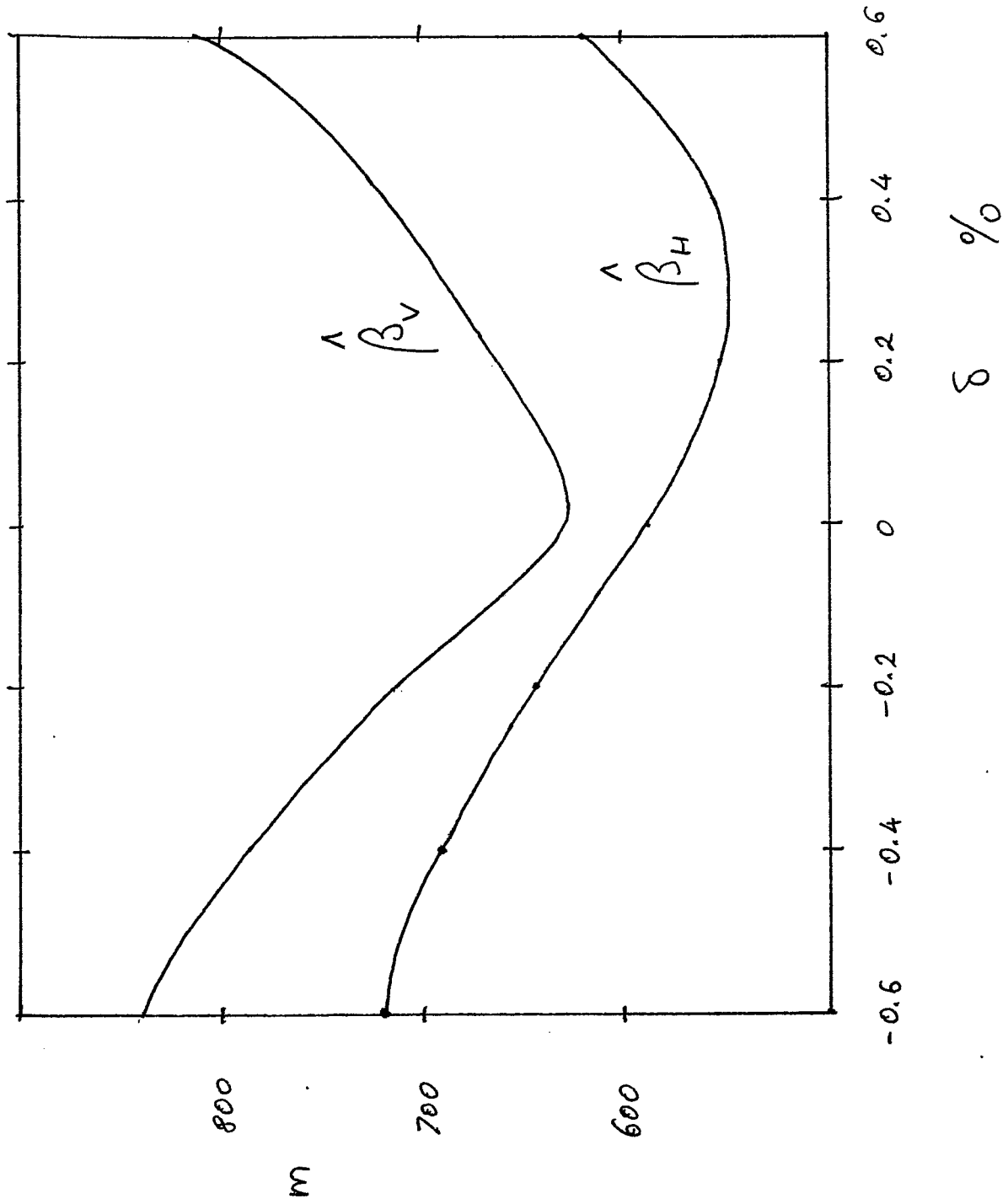
Fig. 33 Variation of β_{max} with Momentum.
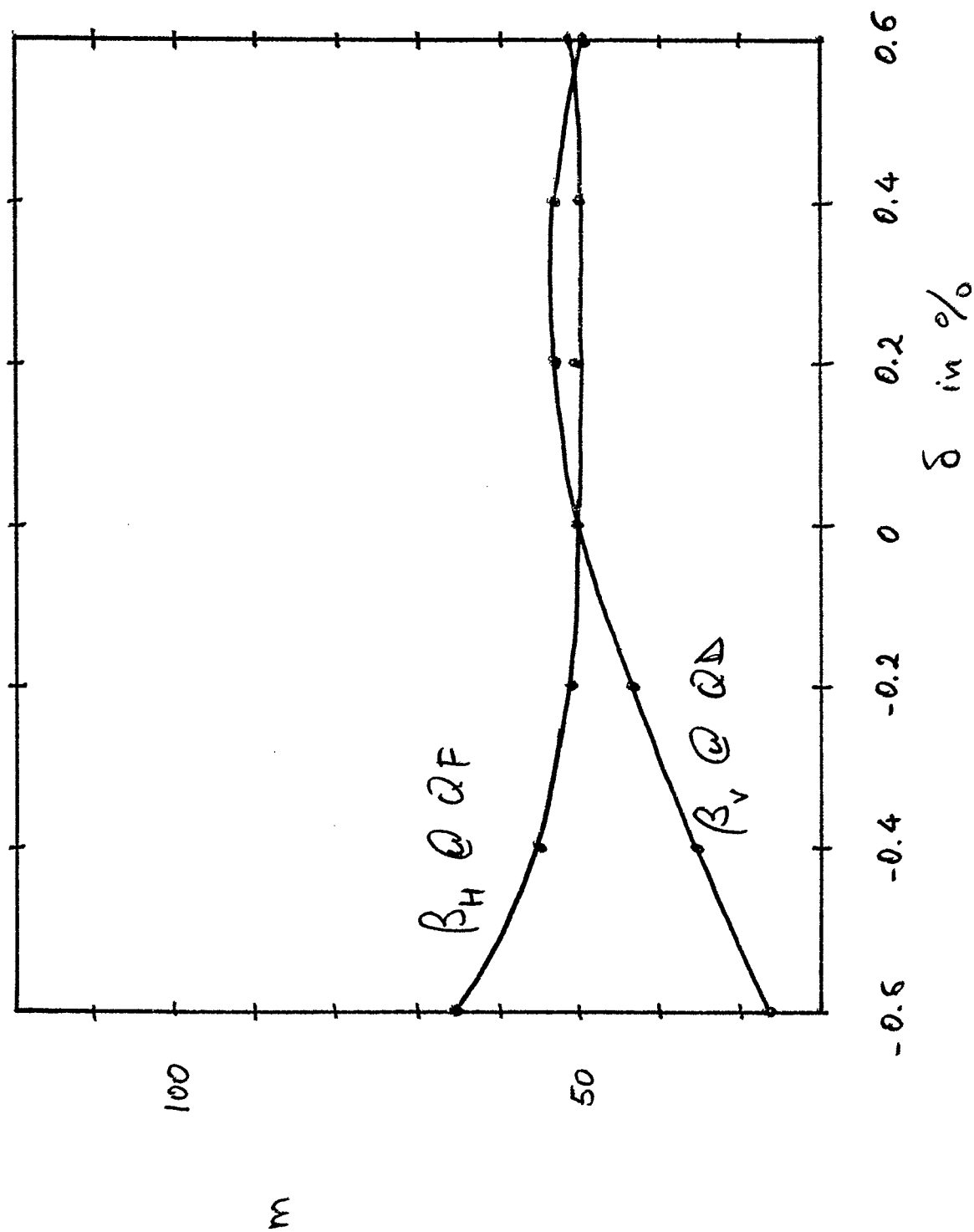
Fig. 34   Variation of β-Functions in the Arcs with Momentum.
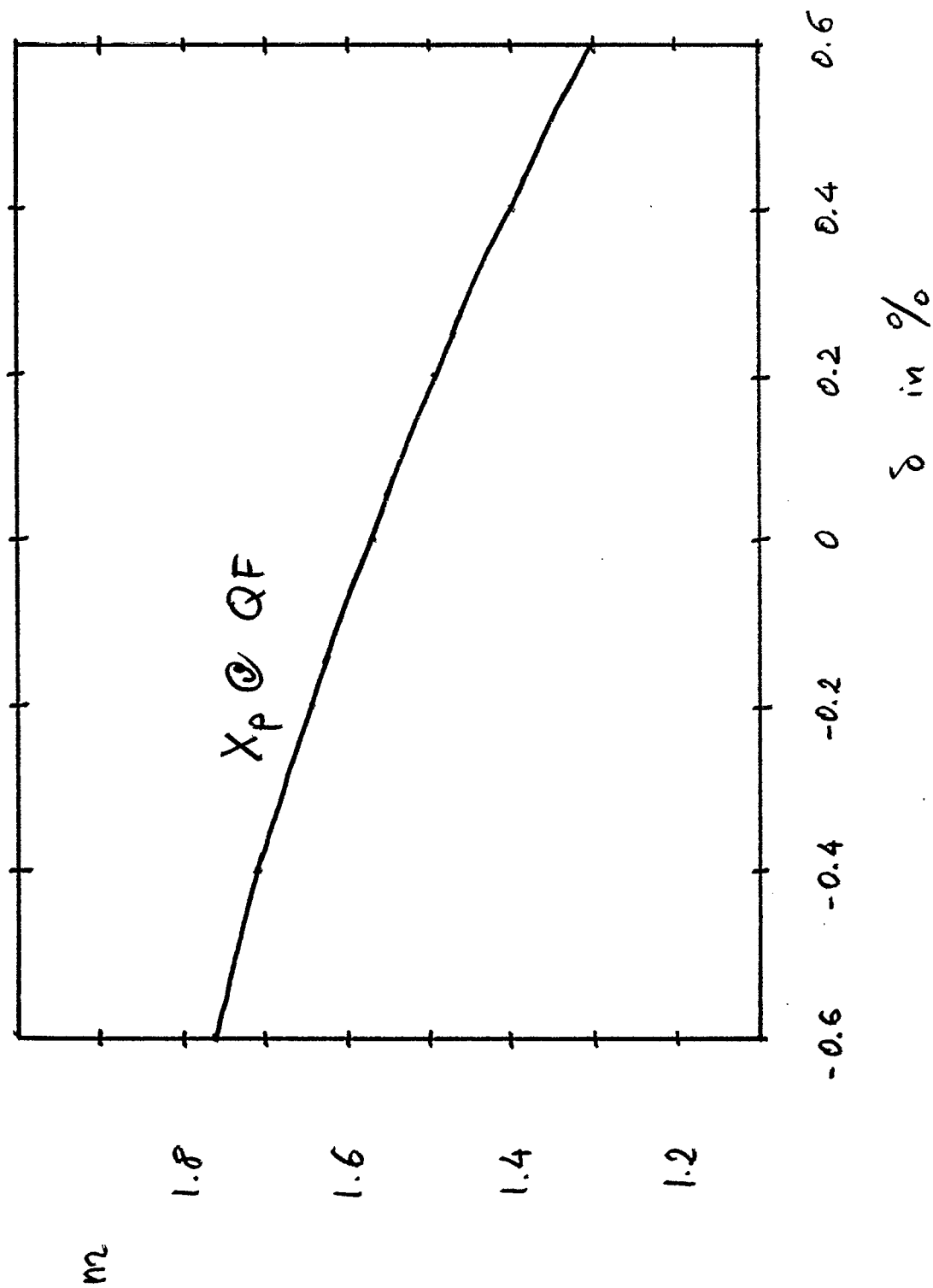
Fig. 35   Variation of Dispersion in the Arcs with Momentum.

72
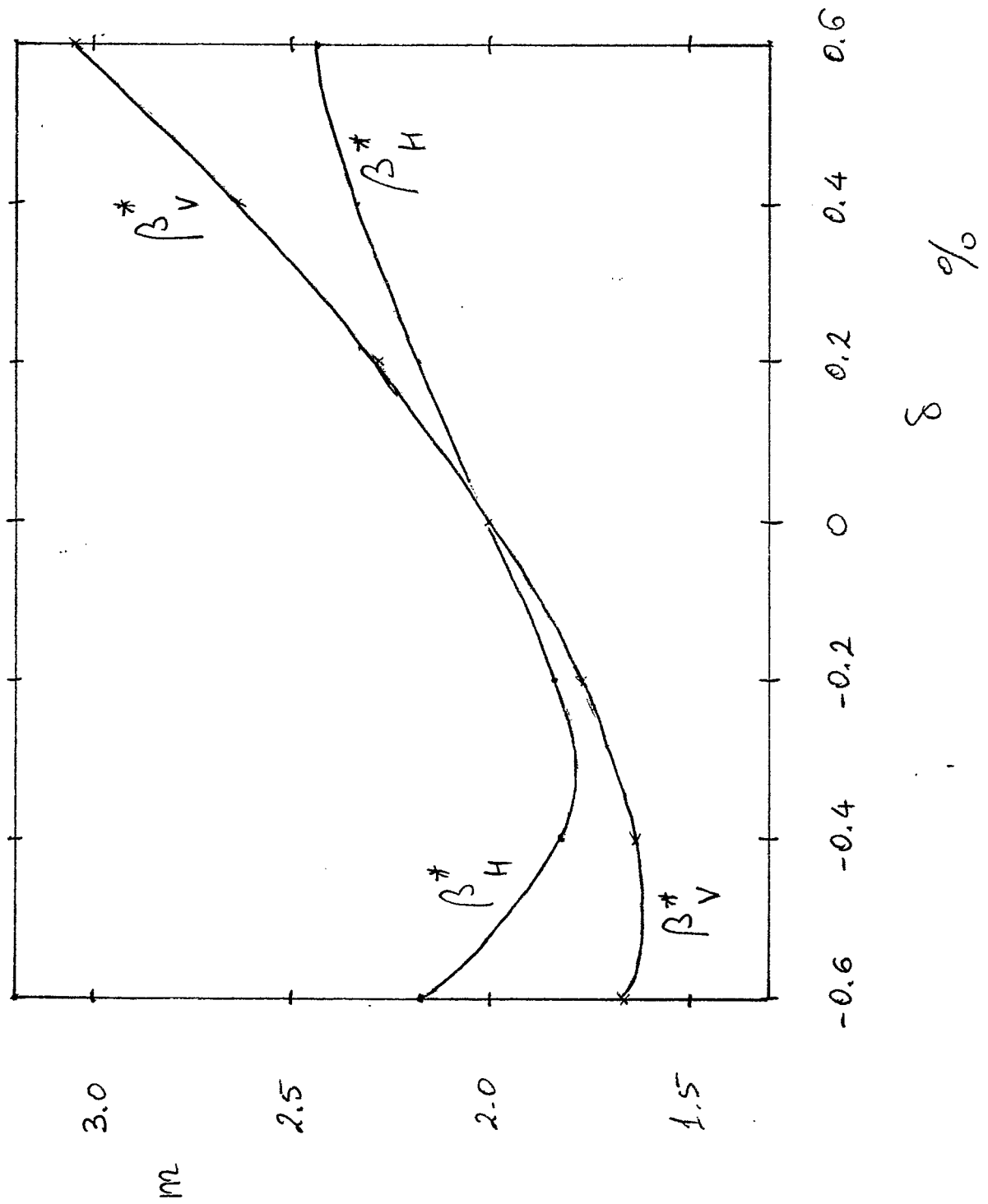
Fig. 36   Variation of β^*-Values with Momentum.
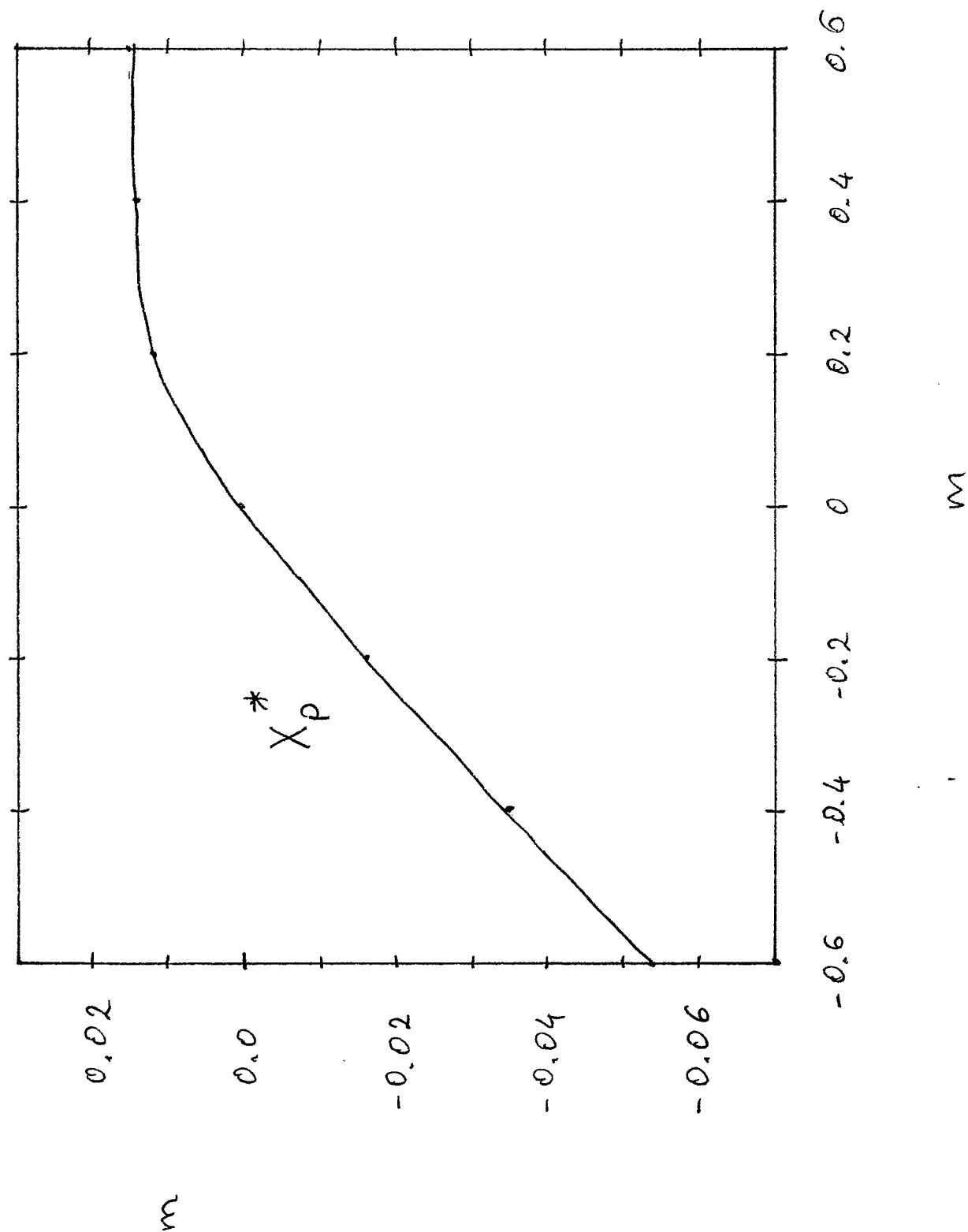
Fig. 37. Variation of Dispersion at the Crossing Point with Momentum.
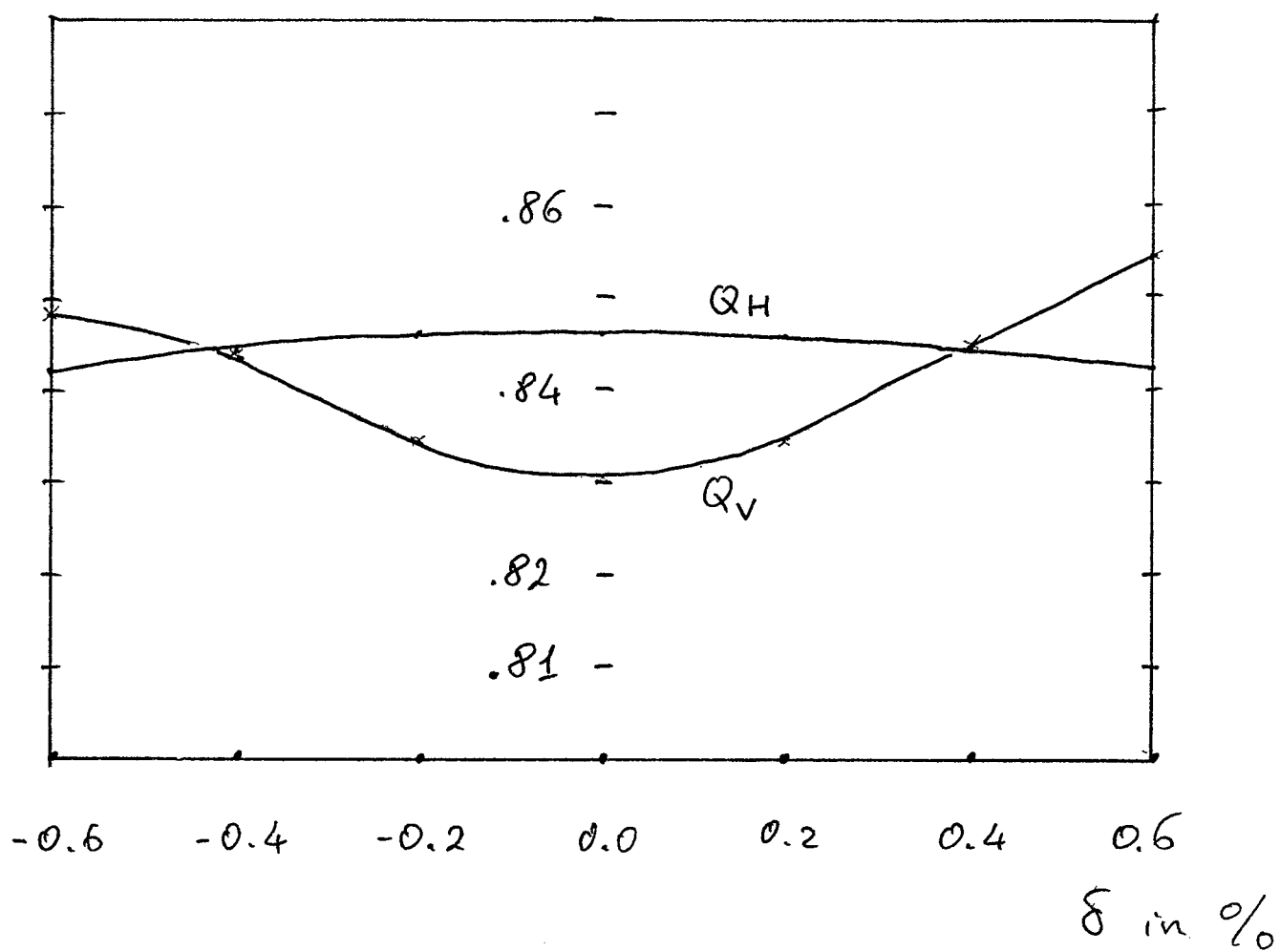
$$Q_H = 33.8462 \qquad \beta^* = 2m$$

$$Q_V = 28.8303$$

Fig. 38   Chromaticities in RHICAGR with Betatron
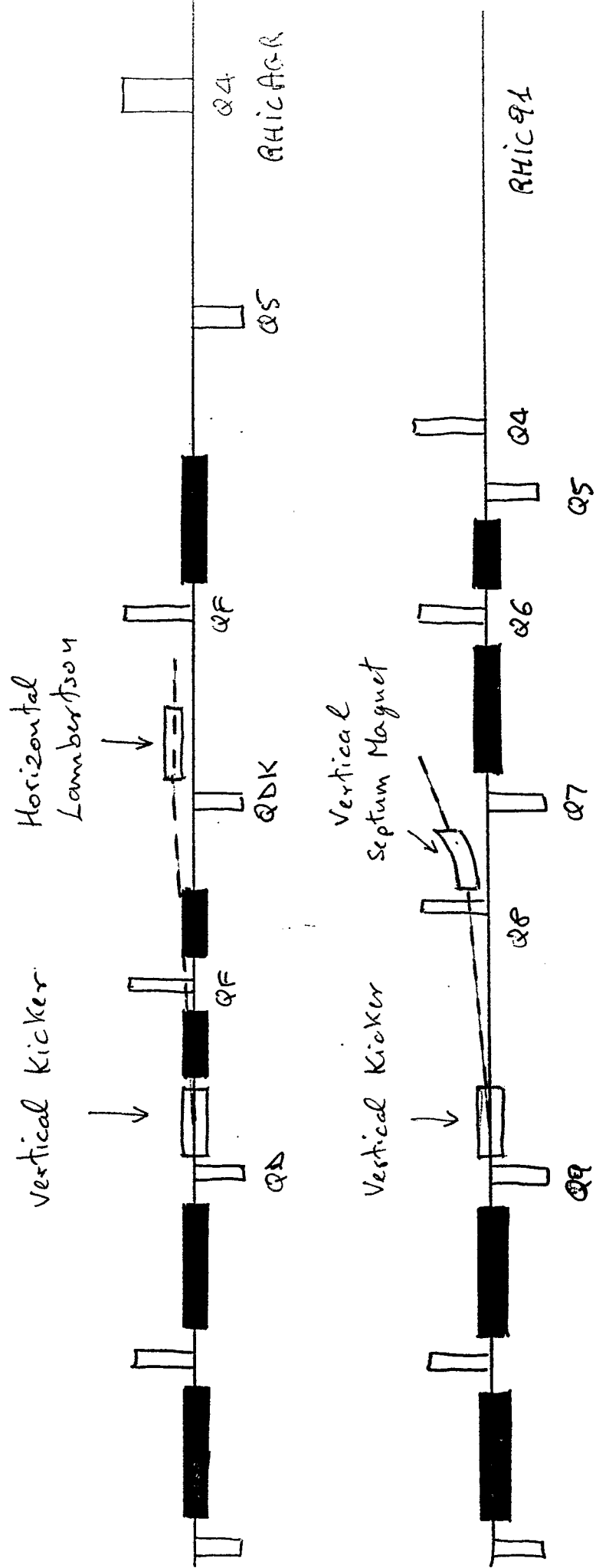Detuning and Unchanged Sextupole Setting.
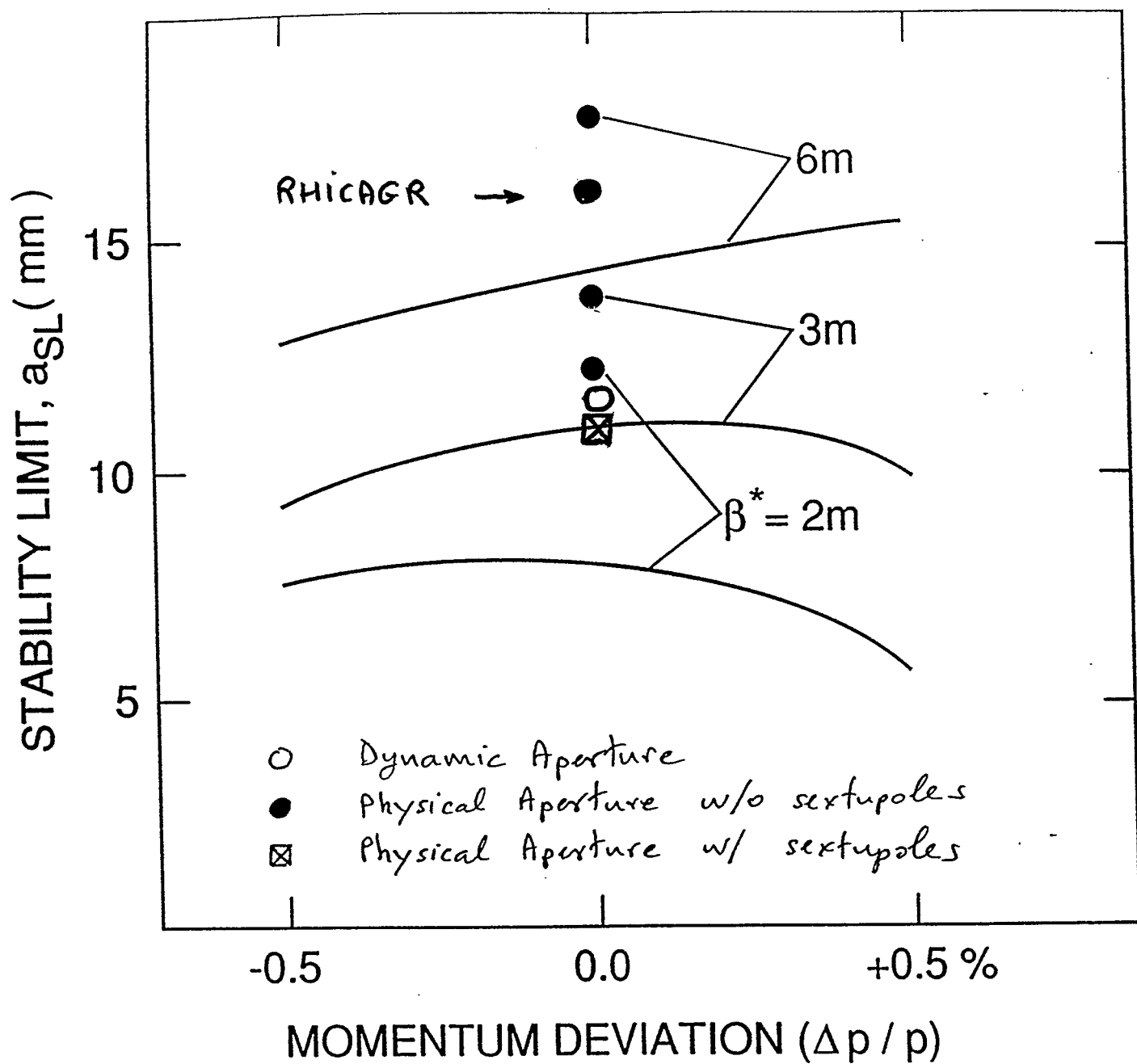
Fig. 39 Comparison of Physical and Dynamical
Aperture between RHICAGR and RHIC91.

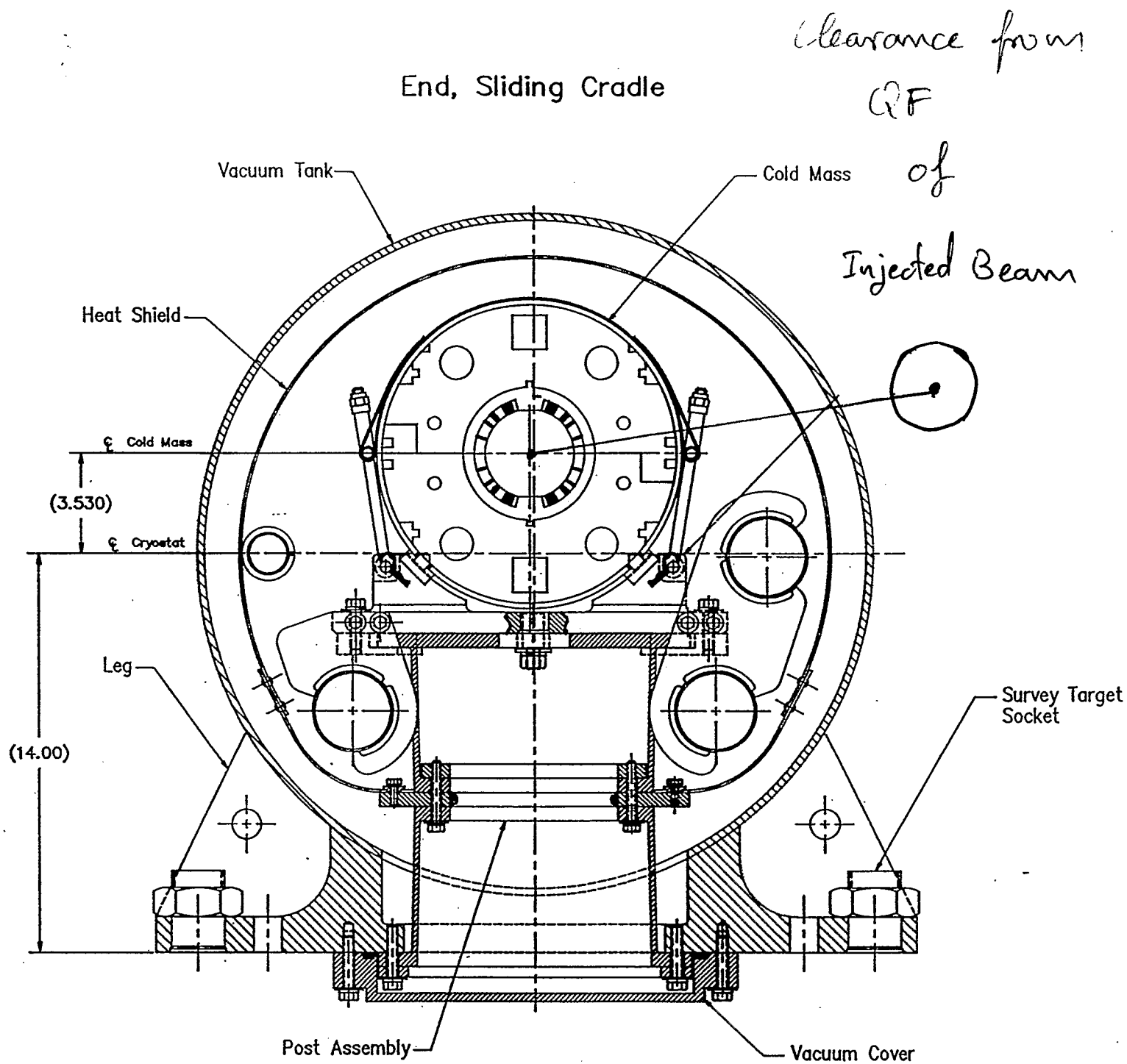Fig. 40   Injection in RHICAGR and RHIC91.

End, Sliding Cradle
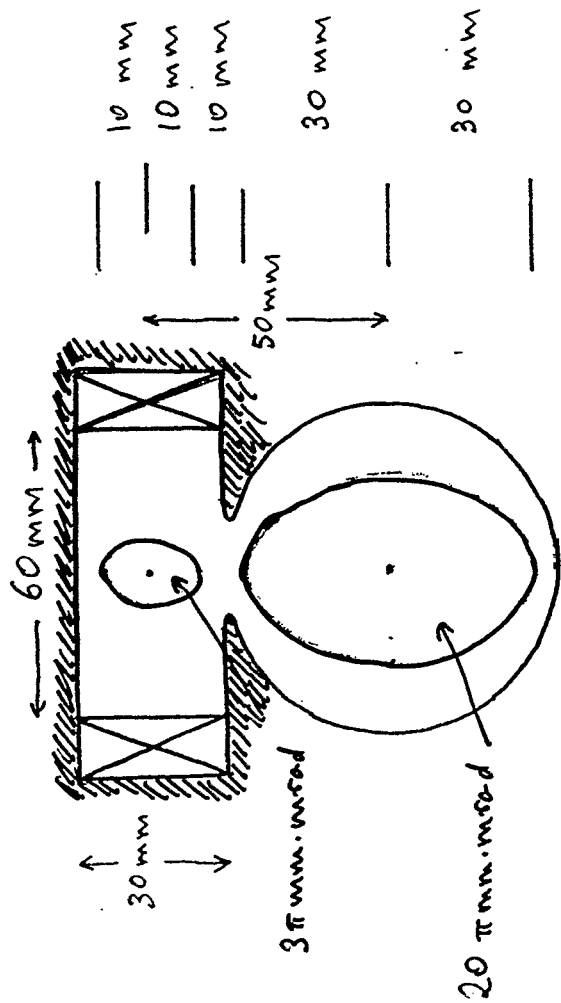
Clearance from QF of Injected Beam

Vacuum Tank

Cold Mass

Heat Shield

₵ Cold Mass

(3.530)

₵ Cryostat

Leg

(14.00)

Survey Target Socket

Post Assembly

Vacuum Cover
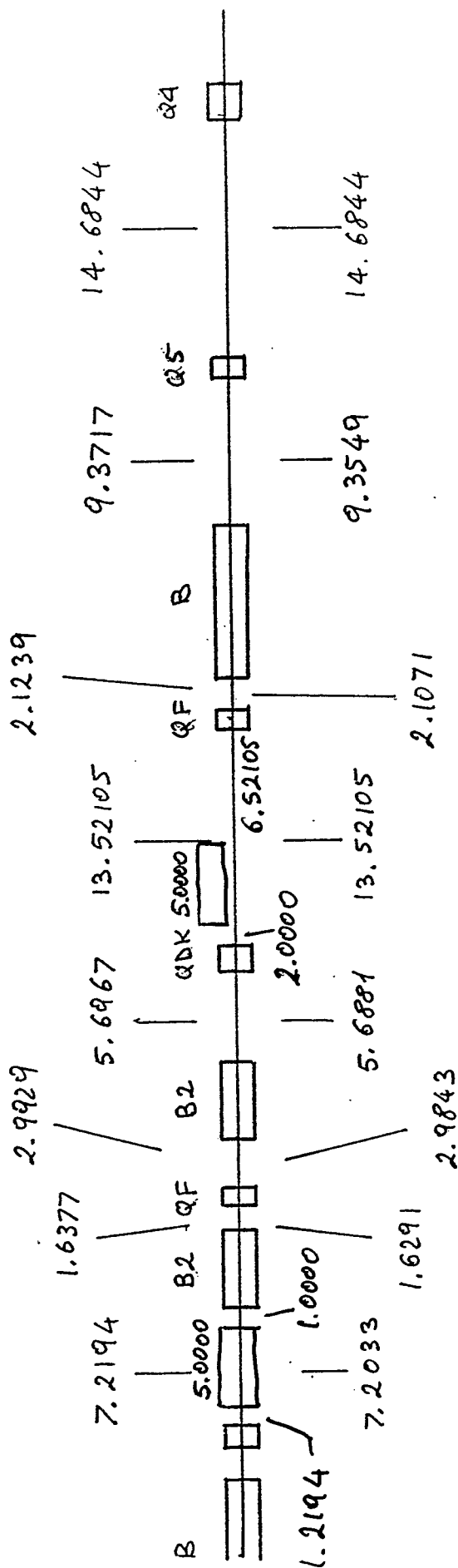
FINISHED ASSEMBLY

Fig. 41   Injected Beam Location Relative to QF
Quadrupole Upstream of Lambertson Magnet.

Fig. 42   Details of the RHICAGR Lattice around Injection.

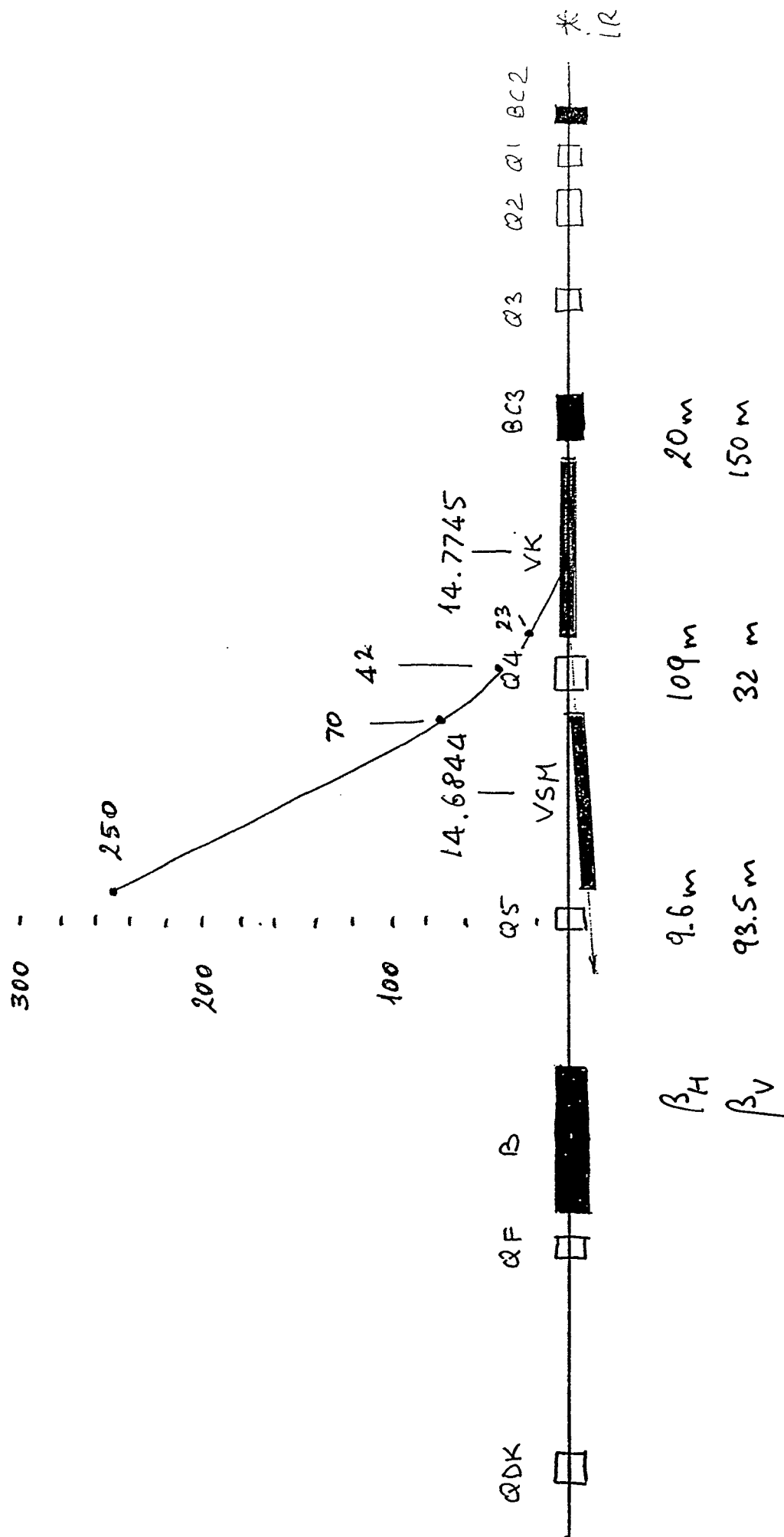Kicker & Lambertson : Warm

All Other Magnets : Cold

10 mm
10 mm
10 mm
30 mm
30 mm

50 mm

60 mm

30 mm

3 π mm.mrad

20 π mm.mrad

Fig. 43   Scheme of Vertical Beam Abort from RHICAGR.

End, Sliding Cradle

Vacuum Tank

Cold Mass

250mm

Heat Shield

Cradle Assembly

₵ Cold Mass

(3.530)

₵ Cryostat

Leg

Survey Target Socket

(14.00)

Post Assembly

Vacuum Cover

FINISHED ASSEMBLY
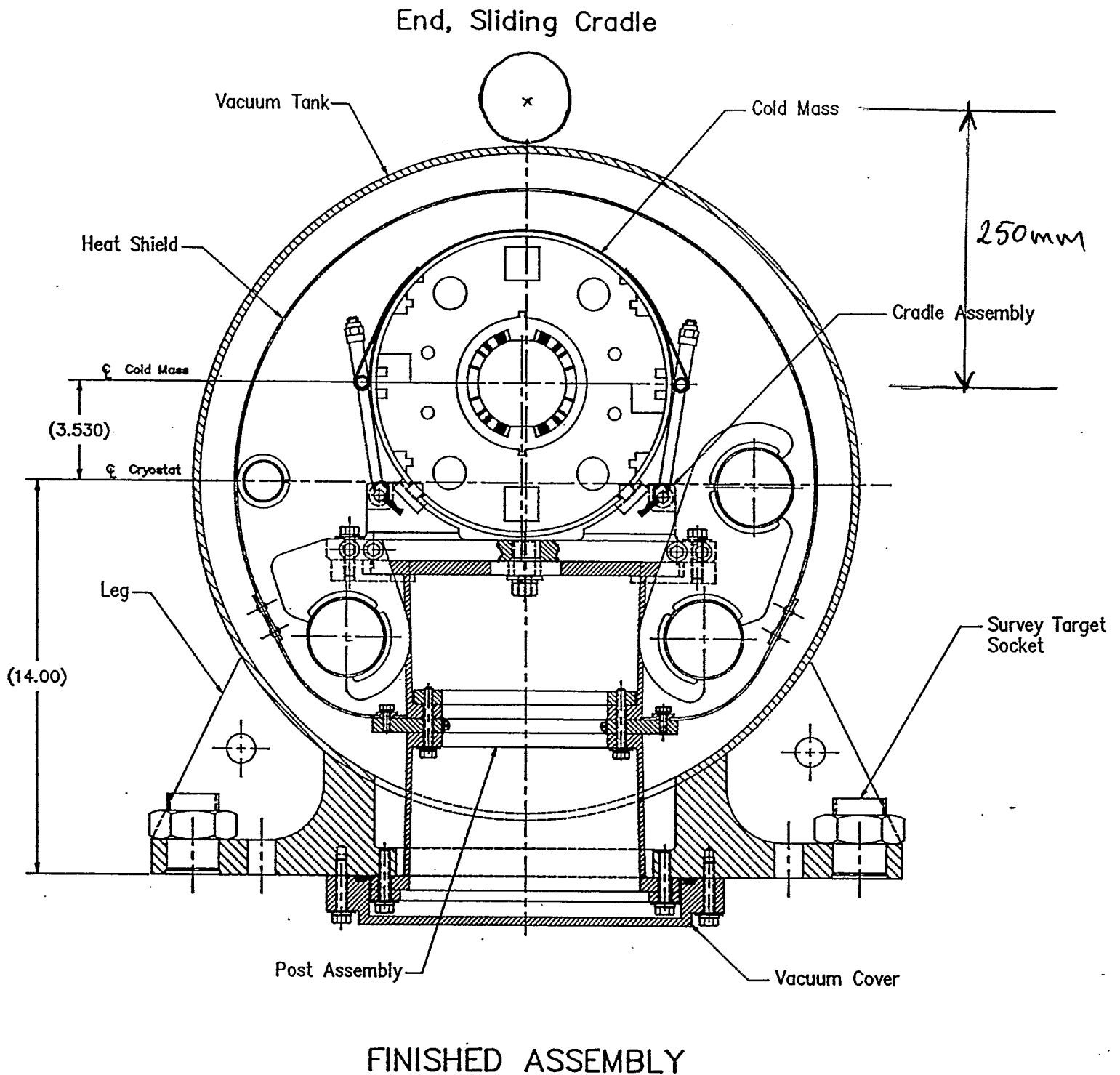
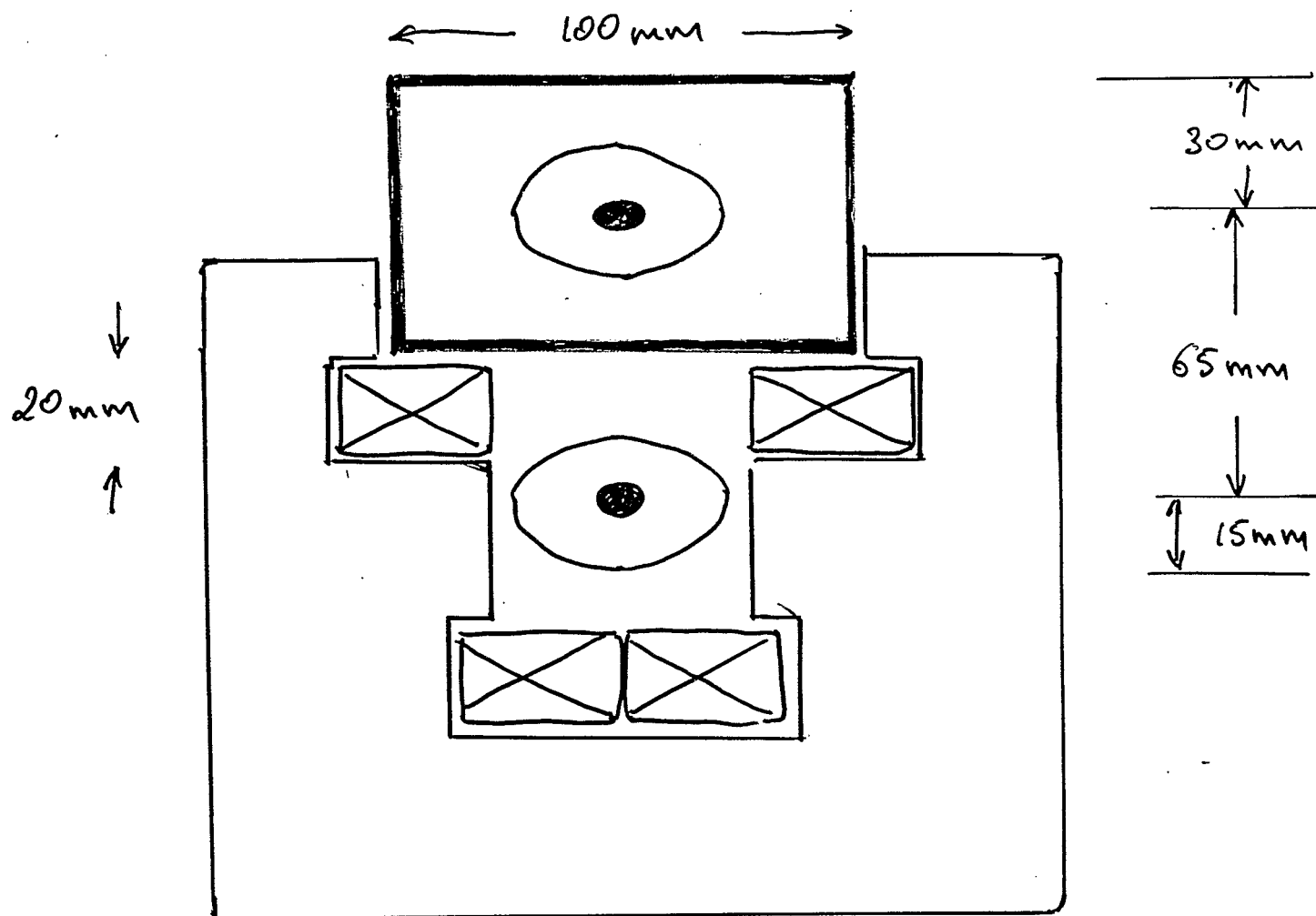Fig. 44 Relative Location of the Aborted Beam with
respect to Q5 in RHICAGR.

Fig. 45   A C-Magnet as Extraction Device
          Surrounding Vacuum Chamber.